Elsevier Editorial System(tm) for Environmental Research

Manuscript Draft

Manuscript Number: ER-16-970R1

Title: Chronic toxicity effects of ZnSO4 and ZnO nanoparticles in Daphnia magna

Article Type: Research paper

Section/Category: Ecotoxicology

Keywords: Toxicity; Ionic Zinc; Zinc oxide; Daphnia magna; TEM.

Corresponding Author: Dr. Renato Bacchetta,

Corresponding Author's Institution: Università degli Studi di Milano

First Author: Renato Bacchetta

Order of Authors: Renato Bacchetta; Nadia Santo; Marcello Marelli; Greta Nosengo; Paolo Tremolada

Abstract: The chronic toxicity of ZnSO4 and ZnO nanoparticles has been studied in Daphnia magna also considering the life cycle parameters beyond the standard 21-day exposure time. Specimens have been individually followed until the natural end of their life, and some of them sampled for microscopic analyses at 48 hours, 9 and 21 days. Despite the low level of exposure (0.3 mg Zn/L), ultrastructural analyses of the midgut epithelial cells revealed efficient internalization of nanoparticles between 48h and 9d, and translocation to other tissues as well. At 21d, the most affected fields have been recorded for both compounds; in particular samples exposed to ZnO nanoparticles showed swelling of mitochondria, while those exposed to ZnSO4 had a great number of autophagy vacuoles. The life cycle parameters resulted altered as well, with a significant inhibition of reproduction in both groups, when compared to controls. After the 21-day exposure, some interesting results were obtained: animals, previously exposed to nanoZnO at low concentrations, showed a complete recovery of the full reproduction potential, while those previously exposed to ZnSO4 presented a dose-dependent and compound-specific reduction in lifespan. Based on the results from the present research and the effects of the same chemicals at higher doses, it can be concluded that the soluble form plays a key role in ZnO nanoparticle cytotoxicity, and that the nanoparticulate form is able to locally increase the amount of Zn inside the cell, even within the ovary. It's worth noting that ZnO nanoparticles have been internalized despite the very low concentration used: this raises concern about the possible environmental implications which may derive from their use, and which in turn must be carefully considered.

Response to Reviewers: Reviewer #1

About the chapter: “Life cycle behaviour”
As suggested we have re-written the whole chapter and integrated it with new data and a new Figure (Fig. 1). We have also put in the Supplementary

Material Section two additional Tables with all the recorded life cycle parameters (Table S1 and Table S2).

About the increased reproduction rate, P10
We added new data and explanations in the text (see also the new Table 1).

About the correlation between viability and fertility, P10
As suggested, we removed the original sentence and added a new Figure showing the probabilities of survival for the tested concentrations.

Reviewer #2

About the comparison between ZnO nanoparticles and Zinc salts
The real role of soluble zinc in ZnO NP toxicity is far from being completely understood. Our data suggest that the toxic effects observed by microscopic analyses are mainly due to soluble zinc, thus the assumption made by the Reviewer is legitimate. Indeed, as specified in the manuscript, we believe that the toxicity is mainly due to the high intra-cellular concentration of ions that are released by NPs once inside the cell. We expanded the discussion on this topic and widely discussed this point. In accordance with the literature, we concluded that at low concentrations ZnO NP are more toxic than $ZnSO_4$.

Point 1: About the first highlight
The first highlight stated that $ZnSO_4$ exposure for 48h did not cause any alteration in the midgut cells of D. magna, which appeared with no morphological effects, and very similar to those observed in controls. On the contrary, ZnO exposed samples showed some NPs inside cells, indicating that internalization of material has been occurred. To avoid misunderstanding however we modified the first highlight, removing the last portion of the original sentence.

Point 2: About the measurement of the released ions
The release of ions over time has been performed at three different times: 0, 24 and 48h for both concentrations and compounds, as specified in the Material and Methods, P7. We did not consider additional times since every two days the exposure media were renewed.

Point 3: About the effect due to ions
See above:
“About the comparison between ZnO nanoparticles and Zinc salts”

Point 4: About the effects on daphnids by an indirect toxicity coming from the mothers
As suggested by Referee #1 the paragraph on the life cycle behaviour has been completely re-written, and a new paragraph with the effects on daphnids has been put in the Discussion.

Point 5: About the “dots” in the TEM images
Throughout the manuscript, the composition of what we have described as nanoparticles (dots) has always been confirmed by ESI analysis, thus the real nature of those dots is unquestionable. In the text we put only three fields in which the elemental composition of the NPs is evidenced (Fig. 4), but the ESI analysis has been performed on all samples. Of course such dots are absent in the controls (Fig. 2). The EDX analysis was performed on NPs to assess the purity of the sample (P6, lines 1-3)

Point 6: About the damages observed in mitochondria and the role of oxidative stress
The linkage between oxidative stress and swollen mitochondria is well documented in literature (for ZnO NPs, but also for $ZnSO_4$) and many papers, some of which cited in the text, have clearly demonstrated that this kind of mitochondrial alteration was due to an excessive ROS production. Based on the extensive literature on the topic, we avoid measuring the level of OS also considering the morphological approach used in this paper. Such an approach was used to better compare the present results with those from our previous works, which considered the chronic effects of both nanoZnO and $ZnSO_4$, mainly by an ultrastructural point of view (Santo et al., 2014; Bacchetta et al., 2016). Moreover, in one of our previously published paper (Bacchetta et al., 2014), we demonstrated that the same nanoparticles used in the present research were able to cause OS in the same cellular type here considered (enterocytes). This, allowed us considering that also this time the mechanism of action of these ZnO NPs still remained the same.

Reviewer #3

About the dissolution kinetics of ZnO nanoparticles
Here we paste the same answer given to the Reviewer #1
The release of ions over time has been performed at three different times: 0, 24 and 48h for both concentrations and compounds, as specified in the Material and Methods, P7. We did not consider additional times since every two days the exposure media were renewed.

Abstract - About ZnO NP internalization
What is surprising is that ZnO NPs were internalized despite the very low concentration tested; we underlined this issue since it was never reported before in literature. In the manuscript we discussed this point considering the high solubility of ZnO NPs reported in the few papers available on the topic (P. 15), but in the abstract we would like to maintain the original sentence, avoiding additional integration.

P. 5; About details in the preparation method
We simplified the paragraph removing some sentences.

P. 7; About the dissolution experiments
As suggested, we have revised the paragraph.

P. 13; About intracellular Zinc concentration
What we have proposed in the Discussion (lines 16-49) were speculations about the potential Zinc exposure for gut cells, starting from the mean number of NPs observed into them by EM. Since what we have observed and counted into cells were NPs, we are aware that our calculations are far from giving real measures of soluble zinc into cells, but they have the only purpose to demonstrate the potential burden of soluble zinc for tissues exposed to NPs.

About Figure 3
Here we paste the same answer given to the Reviewer #2
The composition of what we have described as nanoparticles (dots) has always been confirmed by ESI analysis, thus the real nature of those dots is clear. In the text we put only three fields in which the elemental composition of the NPs is evidenced (Fig. 4), but the ESI analysis has been performed on all samples. Of course such dots are absent in the controls (Fig. 2).

About minor comments
- Abstract: We modified the abstract removing the expression “affected fields”
- p. 4, line 40: We removed the “s” to internalization
- p. 21, line 34: We modified citotoxicity in cytotoxicity
- p. 21, line 46: we modified the expression “wild use” in “uncontrolled use”

Responses to Reviewers

Reviewer #1

About the chapter: "Life cycle behaviour"

As suggested we have re-written the whole chapter and integrated it with new data and a new Figure (Fig. 1). We have also put in the Supplementary Material Section two additional Tables with all the recorded life cycle parameters (Table S1 and Table S2).

About the increased reproduction rate, P10

We added new data and explanations in the text (see also the new Table 1).

About the correlation between viability and fertility, P10

As suggested, we removed the original sentence and added a new Figure showing the probabilities of survival for the tested concentrations.

Reviewer #2

About the comparison between ZnO nanoparticles and Zinc salts

The real role of soluble zinc in ZnO NP toxicity is far from being completely understood. Our data suggest that the toxic effects observed by microscopic analyses are mainly due to soluble zinc, thus the assumption made by the Reviewer is legitimate. Indeed, as specified in the manuscript, we believe that the toxicity is mainly due to the high intra-cellular concentration of ions that are released by NPs once inside the cell. We expanded the discussion on this topic and widely discussed this point. In accordance with the literature, we concluded that at low concentrations ZnO NP are more toxic than $ZnSO_4$.

Point 1: About the first highlight

The first highlight stated that $ZnSO_4$ exposure for 48h did not cause any alteration in the midgut cells of *D. magna*, which appeared with no morphological effects, and very similar to those observed in controls. On the contrary, ZnO exposed samples showed some NPs inside cells, indicating that internalization of material has been occurred. To avoid misunderstanding however we modified the first highlight, removing the last portion of the original sentence.

Point 2: About the measurement of the released ions

The release of ions over time has been performed at three different times: 0, 24 and 48h for both concentrations and compounds, as specified in the Material and Methods, P7. We did not consider additional times since every two days the exposure media were renewed.

Point 3: About the effect due to ions

See above:

"About the comparison between ZnO nanoparticles and Zinc salts"

Point 4: About the effects on daphnids by an indirect toxicity coming from the mothers

As suggested by Referee #1 the paragraph on the life cycle behaviour has been completely re-written, and a new paragraph with the effects on daphnids has been put in the Discussion.

Point 5: About the "dots" in the TEM images

Throughout the manuscript, the composition of what we have described as nanoparticles (dots) has always been confirmed by ESI analysis, thus the real nature of those dots is unquestionable. In the text we put only three fields in which the elemental composition of the NPs is evidenced (Fig. 4), but the ESI analysis has been performed on all samples. Of course such dots are absent in the controls (Fig. 2). The EDX analysis was performed on NPs to assess the purity of the sample (P6, lines 1-3)

Point 6: About the damages observed in mitochondria and the role of oxidative stress

The linkage between oxidative stress and swollen mitochondria is well documented in literature (for ZnO NPs, but also for $ZnSO_4$) and many papers, some of which cited in the text, have clearly demonstrated that this kind of mitochondrial alteration was due to an excessive ROS production. Based on the extensive literature on the topic, we avoid measuring the level of OS also considering the morphological approach used in this paper. Such an approach was used to better compare the present results with those from our previous works, which considered the chronic effects of both nanoZnO and $ZnSO_4$, mainly by an ultrastructural point of view (Santo et al., 2014; Bacchetta et al., 2016). Moreover, in one of our previously published paper (Bacchetta et al., 2014), we demonstrated that the same nanoparticles used in the present research were able to cause OS in the same cellular type here considered (enterocytes). This, allowed us considering that also this time the mechanism of action of these ZnO NPs still remained the same.

Reviewer #3

About the dissolution kinetics of ZnO nanoparticles

Here we paste the same answer given to the Reviewer #1

The release of ions over time has been performed at three different times: 0, 24 and 48h for both concentrations and compounds, as specified in the Material and Methods, P7. We did not consider additional times since every two days the exposure media were renewed.

Abstract - About ZnO NP internalization

What is surprising is that ZnO NPs were internalized despite the very low concentration tested; we underlined this issue since it was never reported before in literature. In the manuscript we discussed this point considering the high solubility of ZnO NPs reported in the few papers available on the topic (P. 15), but in the abstract we would like to maintain the original sentence, avoiding additional integration.

P. 5; About details in the preparation method

We simplified the paragraph removing some sentences.

P. 7; About the dissolution experiments

As suggested, we have revised the paragraph.

P. 13; About intracellular Zinc concentration

What we have proposed in the Discussion (lines 16-49) were speculations about the potential Zinc exposure for gut cells, starting from the mean number of NPs observed into them by EM. Since what we have observed and counted into cells were NPs, we are aware that our calculations are far from giving real measures of soluble zinc into cells, but they have the only purpose to demonstrate the potential burden of soluble zinc for tissues exposed to NPs.

About Figure 3

Here we paste the same answer given to the Reviewer #2

The composition of what we have described as nanoparticles (dots) has always been confirmed by ESI analysis, thus the real nature of those dots is clear. In the text we put only three fields in which the elemental composition of the NPs is evidenced (Fig. 4), but the ESI analysis has been performed on all samples. Of course such dots are absent in the controls (Fig. 2).

About minor comments

- Abstract: We modified the abstract removing the expression “affected fields”
- p. 4, line 40: We removed the “s” to internalization
- p. 21, line 34: We modified citotoxicity in cytotoxicity
- p. 21, line 46: we modified the expression “wild use” in “uncontrolled use”

Highlights

- Internalization of nanoparticles occurred within 48h ~~while $ZnSO_4$ had no effect~~
- Life cycle parameters were altered by 0.1 mg Zn/L for ZnO and $ZnSO_4$
- Chronic exposure to ZnO nanoparticles caused swelling of mitochondria
- Chronic exposure to $ZnSO_4$ caused a great number of autophagy vacuoles
- The soluble form plays a key role in ZnO nanoparticle cytotoxicity

Chronic toxicity effects of $ZnSO_4$ and ZnO nanoparticles in *Daphnia magna*

Renato Bacchetta [a,*], Nadia Santo [a], Marcello Marelli [b], Greta Nosengo [a], Paolo Tremolada [a]

[a] Department of Life Sciences, Università degli Studi di Milano, Via G. Celoria, 26, I-20133 Milan, Italy

[b] CNR-ISTM - Istituto di Scienze e Tecnologie Molecolari, Via C. Golgi, 19, I-20133 Milan, Italy

** Corresponding author*.

Renato Bacchetta

Tel: +39 02 503 14783; fax: +39 02 503 14781

E-mail address: renato.bacchetta@unimi.it

Department of Life Sciences

Università degli Studi di Milano

Via G. Celoria, 26

I-20133 Milan, Italy

Abstract

The chronic toxicity of $ZnSO_4$ and ZnO nanoparticles has been studied in *Daphnia magna* also considering the life cycle parameters beyond the standard 21-day exposure time. Specimens have been individually followed until the natural end of their life, and some of them sampled for microscopic analyses at 48 hours, 9 and 21 days. Despite the low level of exposure (0.3 mg Zn/L), ultrastructural analyses of the midgut epithelial cells revealed efficient internalization of nanoparticles between 48h and 9d, and translocation to other tissues as well. At 21d, the most affected fields have been recorded for both compounds; in particular samples exposed to ZnO nanoparticles showed swelling of mitochondria, while those exposed to $ZnSO_4$ had a great number of autophagy vacuoles. The life cycle parameters resulted altered as well, with a significant inhibition of reproduction in both groups, when compared to controls. After the 21-day exposure, some interesting results were obtained: animals, previously exposed to nanoZnO at low concentrations, showed a complete recovery of the full reproduction potential, while those previously exposed to $ZnSO_4$ presented a dose-dependent and compound-specific reduction in lifespan. Based on the results from the present research and the effects of the same chemicals at higher doses, it can be concluded that the soluble form plays a key role in ZnO nanoparticle cytotoxicity, and that the nanoparticulate form is able to locally increase the amount of Zn inside the cell, even within the ovary. It's worth noting that ZnO nanoparticles have been internalized despite the very low concentration used: this raises concern about the possible environmental implications which may derive from their use, and which in turn must be carefully considered.

Keywords: Toxicity; Ionic Zinc; Zinc oxide; Daphnia magna; TEM.

1. Introduction

Toxicological properties of nanoparticles (NPs) are currently under investigation because of their large applications in industry and common-use products. Due to their well-known chemico-physical characteristics (Vaseem et al., 2010), ZnO NPs are among the most used NPs and consequently subjected to be dispersed in the environment (Kahru and Dubourguier, 2010). In the last years, the ecotoxicity of NPs and in particular the effects of ZnO on organisms have been largely studied (Farre et al., 2009). Toxicological data of ZnO NPs revealed a wide range of sensitivity among species: algae were the most sensible with EC_{50} values around 0.05 mg Zn/L (Aruoja et al., 2009; Franklin et al., 2007), while bacteria and nematoda showed EC_{50} values as high as 800 mg Zn/L (Heinlaan et al., 2008; Wang et al., 2009). Protozoa, crustacean and fish showed intermediate EC_{50s}, ranging from less than 1 mg Zn/L (Wiench et al., 2009) up to 18 mg Zn/L (Bai et al., 2010). Nevertheless, the question on the relative contribution to toxicity of the dissolved ions, as well as their action mechanisms in NP cytotoxicity still remained open. Recent studies have begun considering the different contribution to the overall toxicity of the different forms in metal oxide NPs; it is well known in fact that the overall toxicity of a given NP (Tox_{tot}) is the result of the toxicity of the NP itself (Tox_{part}) and that from the solubilized ion (Tox_{ion}). (Xiao et al., 2015) measured the acute toxicity of ZnO NPs in *Daphnia magna*, considering the contribution of the dissolved ions (Tox_{ion}) after centrifugation and filtration, and concluded that most of the toxicity was due to NPs, being the Tox_{ion} contribution around 31%. The same authors showed that the internal concentration of Zn was proportional to the concentration of ZnO NPs administered to daphnids. Moreover, they observed that at high NP concentrations the Tox_{part} played a dominant role, while at low NP concentrations, Tox_{ion} overshadowed the effects of NPs. Several authors affirmed that in the exposure medium a large fraction of NPs rapidly dissolves (Adam et al., 2014; Xiao et al., 2015), while others, measuring very low levels of dissolved ions in the medium, concluded that the dissolution can happen, but mainly inside the cells after NP internalization (Santo et al., 2014). Discrepancies in the percentages of dissolved ion amounts are likely due to the NPs concentration relatively to the equilibrium solubility of ZnO NPs, which is at the mg/L level (David et al., 2012), and also to the combined effects exerted by NP characteristics (presence of coatings, particle size) and exposure medium (ionic strength and pH). Although reasons may be different, depending on NPs and experimental conditions, the majority of authors agree that ZnO NPs toxicity

can be largely attributed to the dissolved fraction, independently from where it happens: in the exposure medium or inside the cell (Adam et al., 2014; Adam et al., 2015; Heinlaan et al., 2008; Santo et al., 2014).

Contrary to acute toxicity, chronic toxicity of ZnO NPs is less studied and more realistic, since generally it happens below 1 mg/L. At low concentrations, the NP behavior can be different and primary internalization and toxicity mechanisms can be better studied with respect to acute toxicity. Only three studies have considered the chronic toxicity of ZnO NPs on *D. magna.* (Zhao et al., 2012) reported very low NOEC (no observed effect concentration) and LOEC (lowest observed effect concentration) values (0.0006 and 0.003 mg Zn/L, respectively), in comparison to the higher values found by (Adam et al., 2014) (0.058 and 0.131 mg Zn/L, respectively) and by (Lopes et al., 2014), who reported a LOEC value of 0.125 mg Zn/L. (Adam et al., 2014) obsereved similar chronic effects on growth, reproduction and accumulation for the ZnO nanoparticles ($EC_{10,\ 20,\ 50}$ of 0.030, 0.049, 0.112 mg Zn/l, respectively) and the $ZnCl_2$ ($EC_{10,\ 20,\ 50}$ of 0.014, 0.027, 0.082 mg Zn/l, respectively), while (Lopes et al., 2014), using differently sized ZnO NPs, showed higher effects for the smaller NPs, but similar effects between the NPs and the dissolved ions. Both these papers concluded that NPs toxicity on *D. magna* reproduction parameters was due to zinc ions.

In the present paper the chronic toxicity of ZnO NPs and that of the soluble zinc salt $ZnSO_4$ have been investigated on *D. magna* by ultrastructural analyses of the midgut cells, during the 21-day chronic test. In addition, the reproduction and life parameters have been recorded and analyzed also after the 21-day exposure, until the end of the whole life cycle (recovery phase). The main questions for the ultrastructural analyses were: *i)* do the internalizations of NPs happen also at low concentrations? and *ii)* does chronic toxicity, with its low level of exposure, cause morphological alterations as well? On the contrary, considering the life cycle assessment: *iii*) are there any differences among treatments? *iv*) are these differences, if any, also evident at the end of the recovery phase? and finally *v*) can the role of (Tox_{part}) and that of (Tox_{ion}) be determined by this double comparison (ultrastructural effects and life cycle behavior)?

2. Material and methods

2.1. Experimental plan

Chronic effects of ZnO NPs and soluble Zn salt, $ZnSO_4$, were analysed during the whole life cycle of *Daphnia magna*. The experimental plan consisted in an exposure phase of 21d, followed by a recovery phase, until the natural end of the life cycle of each animal (around 60d). Exposures were conducted with two concentrations: 0.1 and 0.3 mg Zn/L of nanoZnO and $ZnSO_4$ together with the controls, and samples were fixed for the analyses at three different times: 48h, 9 and 21d.

2.2. ZnO NPs and $ZnSO_4$

Zinc oxide NPs with an advertised particle diameter <50 nm, were purchased from Sigma-Aldrich (Milano, Italy; lot number #MKBD9623V). Stock and exposure suspensions were prepared according to the protocol for nanoparticle dispersions suggested by the PROSPEcT Project in accordance with the agreed OECD WPMN 'Guidance Manual for Sponsors of the OECD Sponsorship Programme for the Testing of Manufacture Nanomaterials'. Briefly, ~~1.867 and 5.601 mg of~~ nanoZnO ~~(which correspond to 1.5 and 4.5 mg of Zn, respectively) were~~ was weighted, initially dispersed in few drops of medium water, then in ~~a final volume of~~ 20 mL. The obtained suspensions were sonicated for 30 second at 20 Khz ± 50 hz, then diluted ~~to 30 mL~~, sonicated again at the same conditions and used to obtain the stock suspensions (50 and 150 mg Zn/L, respectively). ~~Stock suspensions~~ These were always sonicated as above before use. ~~Exposure solutions were prepared by diluting 0.1 mL of the stock solutions in 50 mL of San Benedetto® mineral water in order to obtain the final suspensions of 0.1 and 0.3 mg Zn/L.~~

The Zinc salt, $ZnSO_4$ anhydrous, was purchased from Carlo Erba (Carlo Erba Reagents, Milano, Italy). Two stock solutions of $ZnSO_4$ at a concentration of 50 and 150 mg Zn/L were prepared in deionized water. ~~Exposure groups were prepared by diluting 0.1 mL of the stock solutions in 50 mL of San Benedetto® mineral water in order to obtain the final concentration of 0.1 and 0.3 mg Zn /L.~~

2.3. NP characterization

The effective diameters of more than 500 NPs were randomly evaluated by Transmission Electron Microscopy (TEM) and their size distributions measured by the EsiVision software (Olympus,

Germany). ZnO NPs were additionally analyzed for purity using a Zeiss LEO 1430 Scanning Electron Microscope (SEM), coupled with a Centaurus detector for energy dispersive X-ray spectroscopy analysis (EDX). Dynamic Light Scattering (DLS) was used to characterize the hydrodynamic behavior of the NPs and their extent of aggregation in the same water used for the animal exposure tests, and the Z-potential was registered with a Malvern Nanosizer ZS, (Malvern, UK). Data about the NP characterization are available in (Santo et al., 2014).

2.4. Test species

The freshwater crustacean *Daphnia magna* Straus, originally obtained from the Istituto Superiore di Sanità (ISS, Roma, Italy) and maintained by the authors at the University of Milan, was used as test species. Specimens (30 ind/L) were cultured in a commercial mineral water (San Benedetto®, whose chemico-physical parameters were: conductivity 415 µS cm^{-1} at 20°C, pH 7.42, 301 mg/L HCO_3^-, 48.6 mg/L Ca^{2+}, 28.2 mg/L Mg^{2+}). Cultured daphnids were fed a suspension of the unicellular green alga *Pseudokirchneriella subcapitata* (0- to 8-day-old daphnids: 8 x 10^6 cells ind^{-1} day^{-1} and from 8-day-old daphnids: 16 x 10^6 cells ind^{-1} day^{-1}) and the yeast *Saccharomyces cerevisiae* (15 x 10^6 cells mL^{-1}), three times a week. The culture medium was renewed and offspring discarded three times a week. The breeding cultures were renewed every 5/6 weeks and replaced with neonatal organisms. Daphnids from the fourth reproduction cycle were taken for culture renewal and for the exposure experiments. Culture and exposure solutions were maintained at 20.5 ± 0.5 °C under a 16 h light: 8 h dark photoperiod. According to Frey (Frey, 1982), the above conditions assure continuous amictic parthenogenetic reproduction in cultures. Algae were cultured in ISO 8692:1989 medium within a 2L flask at 20 ± 2°C under continuous light and shaken by bubbling air. Algae were harvested during their exponential growth and left in the dark at 4°C for sedimentation for 8 days. After supernatant elimination, cell density of the concentrated algal suspension was determined using a Burker counting chamber under a Zeiss light microscope.

2.5. Chronic toxicity test and recovery phase

The exposure phase was performed in agreement with the standard 21d chronic reproduction test (OECD, 2012). Stock solutions of $ZnSO_4$ and nanoZnO were freshly prepared before the experiments and used for the two exposure concentrations of 0.1 and 0.3 mg Zn/L, as described above. According

to the OECD recommendations, Zinc ion concentrations in $ZnSO_4$ solutions and the amount of Zn solubilized from NPs in the nanoZnO suspensions were measured in duplicates by Inductively Coupled Plasma - Optical Emission Spectrometry, ICP-OES (Thermo Scientific iCAP6300 Duo, Waltham, MA, USA) after preparation, 24h later, and after 48h. Samples for the analytical determination of Zinc concentration in $ZnSO_4$ groups were filtered with 0.2 μm Nalgene syringe filters with Teflon PTFE membranes (Thermo Fisher Scientific, Milano, Italy), acidified to 1% HNO_3 (≥ 69%, traceSELECT for trace analysis, FLUKA, Seelze, Germany) and maintained in the dark at 4°C. ICP-OES analyses were performed at three characteristic wavelengths for Zn (202.548, 206.200 and 213.856 nm) with very consistent results (mean RSD = 2.0 %). Quantifications were performed at 202.548 nm by a 5-points external calibration line (calibration range: from 0.05 to 0.5 mg Zn/L) with the bracketing method. Each determination was repeated 5 times (mean RSD = 0.47 %). The limit of detection was evaluated at 0.0084 mg Zn/L. Measured Zn concentrations in milliQ water, San Benedetto® mineral water (blank reference), and in control samples at 0, 24 and 48h were below this limit. Measured Zn concentrations in exposure media before the experiments were close to the nominal ones (mean difference in percentage = 6.8 %).

To estimate the possible contribution to toxicity of the zinc ions dissolved from ZnO NPs, ZnO suspensions were ultrafiltered using centrifuge tubes VIVASPIN 20 with a molecular weight cut off of 10 KDa (Sartorius Stedim Biotech GmbH, Goettingen, Germany) in a swing out Eppendorf 5804 R centrifuge (Eppendorf Italia, Milano, Italy) running at 4000 g for 15 min. Filtrates were acidified to 1% HNO_3 and stored at 4°C in dark.

For each treatment group, 15 or 20 replicates of 1 daphnid (<24h) were used. The exposures were conducted in glass beakers containing 50 mL of test medium. The number of replicates was higher than that required by the OECD protocol (n = 10), in order to guarantee a sufficient number of samples at the end of the 21d exposure time, considering those specimens to be fixed for the microscopic analyses at 48h, 9 and 21d. During the exposure phase, daphnids were transferred every 2 days to clean glass beakers filled with freshly prepared medium and fed with *P. subcapitata* and *S. cerevisiae* as indicated above.

At 21 days, the total number of living offspring and mothers were counted in order to match the OECD requirements. The following recovery phase started the 21st day and continued until the end of the life

cycle for each animal. During the recovery phase no exposure to nanoZnO or $ZnSO_4$ was performed and specimens were fed as specified above.

During the exposure and recovery phases, all the experimental groups were maintained at 20.5 ± 0.5 °C under a 16 h light: 8h dark photoperiod and the number of living, immobile and dead offspring were recorded daily. Animals unable to swim within 15 s of gentle agitation of the test container were considered immobile, while those whose heartbeats have stopped were considered dead.

2.6. Light and electron microscopy

Specimens for histological and ultrastructural analyses were randomly selected and fixed in a mixture of 2% paraformaldehyde and 2.5% glutaraldehyde in 0.1 M sodium cacodylate buffered solution at pH 7.4. After washes in the same buffer, daphnids were post-fixed in 1% OsO_4 for 1 h in dark condition, dehydrated in a graded ethanol series and finally in 100% propylene oxide. Infiltration was subsequently performed with propylene oxide and resin (Araldite-Epon) at volumetric proportions of 2:1 for 1.5 h and 1:1 overnight. Daphnids were then embedded in 100% pure resin for 5 h, and polymerization was performed at 60°C for 48h. Sectioning was performed using an Ultracut E microtome (Reichert, Austria): semithin sections of about 1µm were collected onto microscope slides and stained with 1% toluidine blue to select the region of interest. The histological analysis was performed on semithin sections of 0.5 µm from 5 specimens from each treatment group, control included. For the ultrastructural analysis, 15-20 ultrathin sections of about 60/70 nm from the midgut of each sample were collected on 600-mesh uncoated copper grids. Due to the very low level of exposure and in order to maximize the possibility of evidencing cellular damages in the samples, only the 0.3 mg Zn/L groups (nanoZnO and $ZnSO_4$) have been considered for the ultrastructural analyses and 3 daphnids at 48h, 4 at 9d and 5 at 21d from each experimental group, control included, have been processed for a total of 36 samples analyzed. All thin sections were not counterstained and observed with a Zeiss LEO 912ab Energy Filtering TEM operating at 120 kV. Digital images were acquired using a CCD-BM/1K system operating with the ESI vision software AnalySIS (Soft Imaging Systems, Muenster, Germany).

2.7. Data analyses and statistics

The following reproductive parameters were calculated during the exposure and recovery phases:

total number of live offspring per female, total number of immobile/dead offspring per female, time to first broad per female and number of broads per female. From those parameters, mean broad size (mean number of offspring per broad) and mean time between broads were derived. In addition, the eventual early mortality during the experiment (those happened before the 50th days) and the longevity (days from birth for the animal died after the 50th day) was recorded. Reproductive endpoints ~~and longevity~~ among exposed and control specimens were compared in a one-way ANOVA with Bonferroni multiple comparison test and immobile offspring *vs.* control ratio was analysed by Mann-Whitney test. Survival probabilities were calculated according to the Kaplan-Meir method with Log-Rank statistic for testing exposure-control differences. Longevity in controls and treated groups was calculated by probit regression as time at which the 50% of cases died. 95% confidence intervals of mean longevity were reported too. All statistical analyses were performed with SPSS software ver. 15.0. Live offspring *vs.* control difference in percentage was calculated as the mean difference of the total live offspring in treated animals and the mean total live offspring in control, with respect to the mean total live offspring in control ± standard deviation. Immobile offspring *vs.* control ratio was calculated as the mean ratio of the total immobile offspring in treated animals and mean total immobile offspring in control ± standard deviation. Longevity *vs.* control difference in days was calculated as the mean difference of the mother longevity in treated animals and the mean mother longevity in control ± standard deviation. ~~Live offspring number and longevity *vs.* control difference were tested by ANOVA and post-hoc Bonferroni test, and immobile offspring *vs.* control ratio by Mann-Whitney test.~~

3. Results

~~*3.1. Life cycle behaviour*~~

~~At the end of the 21d reproduction test, a mean of 66 ± 10 and 70 ± 12 daphnids per *Daphnia* was recorded in controls for the concentrations of 0.1 and 0.3 mg Zn/L, respectively. Moreover, for both groups no mortality was registered among the mothers in the controls. On the contrary, the tested concentrations for both nanoZnO and $ZnSO_4$ showed significant effects on samples. Even the lowest concentration (0.1 mg Zn/L) showed a total number of live offspring per female significantly lower than that in controls (p=0.001 and p=0.011 for nanoZnO and $ZnSO_4$, respectively). The inhibition~~

percentage was 71 ± 5.2 % and 43 ± 9.5 % for nanoZnO and $ZnSO_4$, respectively, but no statistically significant differences were present between the two chemicals. Also the mean broad size per female was lower than that observed in controls ($p<0.001$ and 0.003 for nanoZnO and $ZnSO_4$, respectively). No significant differences were observed for the time of the first broad, which was slightly retarded for both compounds, and for the number of broad per female, which resulted reduced, especially after nanoZnO exposure.

The recovery phase, from the 21st day until the natural end of the life cycle for each animal, aimed to assess the possible reversibility of the chronic toxicity, but also to highlight the differences in the course of the whole life cycle among the exposed animals. For both concentrations, animals exposed both to nanoZnO and $ZnSO_4$ exhibited an initial phase in which the inhibition was still present: a detoxification phase, which indicatively had the duration of about 20 days. This 3-week-period is followed by a second phase in which the reproduction rate increased, becoming even higher than that of control (effective recovery phase). The length of this second phase was quite different among treatments, depending on both compounds and concentrations. Table 1 summarizes the effects of the two chemicals at the two tested concentrations on the following life cycle parameters: total offspring number, offspring immobilisation/mortality and longevity of the mothers, expressed as differences in respect to control. The longevity of the mothers appeared to be the key parameter for life cycle effects, since it directly affected the number of reproduction cycles. Low longevity (negative difference with control) was associated to low reproduction (negative percentage difference with control), and when longevity was higher than in control (exposure to ZnO NPs at 0.1 mg Zn/L), the reproduction was higher too with significant difference *vs*. control ($p=0.018$). At both concentrations, animals exposed to $ZnSO_4$ exhibited a longevity lower than controls (-3.9 ± 4.0 and -8.5 ± 1.7 days for 0.1 and 0.3 mg Zn/L, respectively). On the contrary, animals exposed to nanoZnO showed a longer longevity than controls only at the lowest concentration (+7.0 ± 2.7 days at 0.1 mg Zn/L). At the highest concentration, the longevity was lower than that in control (-5.2 ± 2.5 days), as well as the whole reproduction (-37 ± 5.4 %). Only at 0.3 mg Zn/L, a relatively high number of immobile daphnids was present in the exposed groups. nanoZnO exposure caused the highest number of immobile daphnids (ten times higher than controls), while $ZnSO_4$ treatment was no significant different from controls, even if four times higher. Immobile daphnids were mainly observed at the end of the exposure period, and in the first detoxification phase.

~~This finding supported the conclusion that the effects on daphnids were not caused by direct toxicity coming from the exposure media, but by an indirect toxicity coming from the mothers. Otherwise the immobilisation of daphnids should have happened during the all exposure phase, and should have stopped after it. The finding of an effect on the offspring at the end of the exposure period, and in the first detoxification phase, supported the hypothesis of an effect mediated from the mothers and determined by an accumulation of NPs during the exposure. To study NP internalisation and to test the hypothesis that the effects observed in the offspring were mediated from the mothers and were determined by the accumulation of NPs during the exposure, light and electron microscopy analyses were performed on the highest concentration (0.3 mg Zn/L), considering three exposure times: 48h, 9 and 21d. This choice was also motivated by the consideration that the highest concentration would allowed us to detect the possible morphological effects at cellular level despite the low level of exposure.~~

3.1. Exposure test and life cycle behaviour

D. magna life cycle was divided into two phases: an exposure phase (0-21 days), when treated groups were exposed to chemicals, and a recovery phase, from day 21 to death. Data were split into two different paragraphs corresponding to the two phases described above. Table 1 reported, for each phase and for the whole life cycle, the number of live and immobile/dead neonates per female, together with the lifespan of all samples. The complete set of parameters was listed in Tables S1 and S2, available in the online version of the paper. During the exposure, no mortality was registered among the mothers in control groups and a mean of 66 ± 10 and 70 ± 12 daphnids per *Daphnia* was recorded in the controls for 0.1 and 0.3 mg Zn/L respectively, thus matching the OECD conditions for the validity of the test. As required by the same guidelines, Zn concentrations (referring to the soluble fraction) were analytically measured in the test medium for both exposure and control batches at 1, 24 and 48 h. The first time (1 h) takes into account the lag time necessary for adding algae, yeast and the test species before the water sampling for determination, and the last time (48 h) corresponds to the time for the renewal of solutions.

As already reported above, soluble Zinc concentrations in the exposure medium after $ZnSO_4$ addition were measured just before animal and food addition (time 0) and were very close to the nominal ones (mean difference of 6.8%). In about 1 h (first sampling after animal and food addition), Zinc

concentrations dropped to 66 and 73% of the nominal ones for 0.1 and 0.3 mg Zn/L, respectively. This decrease was likely due to the adsorption by the test species, but mainly by algae and yeast, which had a high surface area in relation to their mass. These latter were likely the most responsible for the observed decrease, since in previous experiments with $ZnSO_4$, in which *D. magna* has been exposed without food sources, soluble Zn concentrations after 48 h from the chemical addition were near the 80% of the initial mass (Bacchetta et al., 2016). On the contrary, in the present conditions the decrease was evident, especially at the lowest concentration. In fact, the median measured concentrations during the renewal interval (0.022 and 0.16 mg Zn/L) were even lower than the half of the nominal concentrations (0.1 and 0.3 mg Zn/L, respectively). Because of this, the effects observed during exposure and recovery phases, must be related to measured concentrations and not to nominal ones. Anyway, for comparison porpoise with the other compound for which the soluble amount was not the only contamination source, nominal concentrations 0.1 and 0.3 mg Zn/L will be maintained in the text.

After nanoZnO addition, soluble zinc concentrations above LOD were registered only for the highest concentration (0.3 mg Zn/L), while they were below LOD (<0.0084 mg Zn/L which means <8.4% of the initial mass) for the lowest one (0.1 mg Zn/L). When concentrations were measured above LOD, a decreasing concentration trend between 1 and 48 h was observed and again, this was likely due to the absorption by organisms. The initial soluble fraction was 24% of the added nanoparticle mass and the final one was 9.4%, indicating that NPs were only partially solubilized. In previous experiments with the same nanoparticles, the amount of soluble Zinc released by NPs was only 2-5% of the initial Zn mass (Santo et al, 2014), and the soluble fraction remained quite constant during the period between renewals (48 h). Despite these discrepancies, the most important result from these analytical measurements was that most of the nanoZnO mass (around 80%) did not solubilize (at least outside organisms), remaining in the particulate form. This evidence was conformed visually, observing deposition of ZnO NPs in the exposure beakers, and by microscopic analyses, by the observation of many NPs in the gut lumen and inside tissues (as described below).

3.1.1. Exposure phase (0-21 days)

At the lowest concentration, the total number of live offspring per female was significantly lower than in controls ($p=0.001$ and $p=0.011$ for nanoZnO and $ZnSO_4$, respectively), while no statistically significant

differences were present between the two chemicals (Table 1). Also the mean brood size per female was lower in treated groups, but without significant differences in respect to control and between the two compounds (Table S1). Even though slightly retarded for both compounds, no statistically differences were observed in the time of the first brood and in the number of brood per female, which however resulted reduced mainly after nanoZnO exposure (Table S1).

At the highest concentration, the total number of live offspring per female was significantly lower than in controls ($p<0.001$ and significant differences between the two chemicals were present, Table 1). Mean brood size per female and the time to first broad were lower and retarded, respectively for both chemicals *vs*. controls, but with significant difference only for nanoZnO (Table S1). The maximal inhibition percentage was reached after 21 days (71 ± 5.2 % and 43 ± 9.5 % for nanoZnO and $ZnSO_4$, respectively) and, at the highest concentration, a high number of immobile/dead daphnids was observed only in the exposed groups, especially following nanoZnO exposure (Table 1). Interestingly, these specimens were mainly observed at the end of the exposure period and in the first days subsequent to the onset of the recovery phase. All reproduction parameters suggested that ZnO NPs had more adverse effects on *D. magna* reproduction than $ZnSO_4$, even if the concentration of soluble Zn in $ZnSO_4$ groups was near 3-fold higher than that measured in ZnO ones.

3.1.2. Recovery phase (21-end of the life cycle)

The recovery phase started from day 21, with the end of the exposure period, and aimed to assess the possible reversibility of the chronic toxicity. Figure 1 showed the survival probability curves of exposed and control groups. For both concentrations and compounds, longevity of exposed animals *vs.* control was significantly different at Log-Rank test ($p<0.001$).

During the recovery phase, reproduction parameters and longevity showed different results, depending on concentration and compound. Animal previously exposed to 0.1 mg Zn/L of nanoZnO exhibited a significant higher number of live neonates per female than controls (Table 1). The longevity of the mothers was higher too, while time between brood and mean brood size did not differ from controls (Table S2), suggesting that the higher reproduction was due to the higher number of broods because of the longer life (mean number of broods per female was significantly higher than that of control, Table S2). An interesting observation, even if not quantitatively evaluated, concerned the body size of specimens at the beginning of the recovery phase. Samples exposed to $ZnSO_4$ did

not show evident differences if compared to controls, while those exposed to nanoZnO were much smaller than the others. As stated above, this item was not supported by direct measurement; anyway this qualitative observation was confirmed by literature data, as reported later in the discussion.

Animals previously exposed to the lowest concentration of $ZnSO_4$ showed slightly lower longevity than controls (mean difference vs. control of -3.9 ± 4.0 days) and a reproduction not significantly different from controls (Table 1).

In synthesis, animals exposed to nanoZnO and $ZnSO_4$ at the lowest concentration exhibited similar effect during the exposure (partial inhibition of the reproduction efficiency), but later, during the recovery phase, they presented a very different behaviour. In fact, animals previously exposed to nanoZnO showed a higher reproduction than control because of a higher longevity, while animals previously exposed to $ZnSO_4$ presented almost the same reproduction efficiency than control but a slightly lower longevity.

Looking at the highest concentration, animals previously exposed to nanoZnO and $ZnSO_4$ presented some differences too. Specimens previously exposed to nanoZnO showed the highest reproduction inhibition (the lowest total number of live neonates per female and the lowest mean brood size, Table S2), while animals previously exposed to $ZnSO_4$ mainly presented more effects on longevity (mean difference vs. control of -8.5 ± 1.7 days) than on reproduction.

During the whole life cycle, mothers exposed to nanoZnO generated the highest number of immobile/dead daphnids (ten times higher than the controls), while $ZnSO_4$ treatment did not present significant differences *vs.* control, even if the number of immobile/dead daphnids was higher than in controls.

The whole experiment, with the two planned phases, allowed us discovering several interesting aspects of the chronic toxicity of these two chemical species of Zinc. NanoZnO exposure seemed to cause the most severe effects on reproduction, with the highest reduction of the reproduction efficiency and possible effect on neonate vitality at the highest concentration. On the contrary $ZnSO_4$ exposure caused more effects on longevity with respect to reproduction. In fact, during the recovery phase, a significant reduction of longevity was obtained at both concentrations, while the total number of live neonates was not statistically different from that recorded in control (Table 1). This was possible because previously exposed animals presented a slightly lower time-between-broads and a slightly higher mean-broad-size, even if both of them were not statistically different from control (Table S2).

Despite this higher reproduction investment (or maybe because of this), the whole reproduction efficiency (total number of live neonates per female) did not differ from that of control, due to the reduction in longevity.

3.2. Light microscopy study

Based on the obtained results and given the low levels of exposure, we decided to perform histological and ultrastructural studies only at the highest concentration (0.3 mg Zn/L), so to better detect the possible morphological effects at cellular level. Histological analyses have been performed on samples mainly focusing at gut level, since it has previously demonstrated to represent a preferential entry route for nanoparticles and xenobiotics in general (Elder et al., 2009).

At 48h, control samples show a regular absorptive midgut composed by columnar cells of about 15-20µm in height, lying on a thick basal lamina and with an evident border of microvilli, longer in the anterior part of the midgut. Epithelial cells show characteristic nuclei, located either centrally or basally, and with clearly evident nucleoli. In the lumen, some ingested material is visible (algae and yeast at different stages of digestion). The digestive system is surrounded by smooth muscle tissue, namely the gut muscolaris, which encircles the whole length of the midgut, and which is well visible in all the sections (Fig. 2). In the nanoZnO and $ZnSO_4$ samples, no differences have been detected if compared to controls, the epithelial cells of the midgut from the exposed samples showing the same structural and morphologic characteristics of the unexposed ones. All digestive cells from treated samples maintained their structural integrity resulting well adherent each other. Also nuclei and nucleoli are similar to those from controls both in size, position and shape, and microvilli are thick and regularly arranged as well (Fig. 2C-F).

At 9d, the morphological fields observed in all samples do not show any differences if compared to controls. Even at 21d, which according to the OECD guidelines represents the exposure time for the chronic reproduction test in *Daphnia* (OECD, 2012), no significant differences have been detected between controls and the exposed groups. Slightly differences have been observed by comparing the height of the digestive cells in the samples from 21d and 48h, the former being higher than the other. Anyway, no pathological features have been detected by light microscopy, and the general morphology of the digestive cells was preserved, being independent upon kind (nanoZnO and $ZnSO_4$) and time of exposure (48h, 9 and 21d).

3.3. Electron microscopy study

More information was expected by TEM analyses, also considering the possibility of recording NPs inside *D. magna* tissues, despite the very low level of exposure. Additionally, considering that no differences between treated and unexposed samples have been recorded by light microscopy, detailed analyses were necessary to compare the possible adverse effects of nanoZnO and $ZnSO_4$ on samples.

Ultrathin sections from controls at 48h, 9 and 21 days showed the typical enterocyte structure, which agreed with the classic description reported by (Quaglia et al., 1976; Santo et al., 2014; Schultz and Kennedy, 1976). Cells showed a well-developed brush border and a cytoplasm rich in organelles, such as mitochondria, endoplasmic reticulum, Golgi apparatus and lysosomes. The numerous mitochondria presented compact and well characterized cristae, and very interestingly, beside mitochondria, a number of others organelles of around 1μm diameter were observed at any time. These structures, more numerous at 9 and 21d than at 48h, showed an inner system of membranes, thus we named them as “lamellar organelles”. They were surprisingly similar to chloroplasts. Indeed the presence of chloroplasts inside the digestive cells of *Daphnia* spp. has already been reported (Chang and Jenkins, 2000). Anyway this very interesting issue was no longer discussed here, since it needed and was worthy of more specific analyses. Figure 3 showed some fields of midgut cells from 21d control samples.

Samples exposed to ZnO NPs showed a general integrity of the midgut enterocytes and little differences have been detected among 48h, 9 and 21d samples. In 48h samples, few ZnO NPs have been observed in the lumen and inside the midgut cells. The number of NPs into epithelial cells increased in 9 and in 21d samples. According to (Mayhew et al., 2009), the average frequency of NPs in cells was calculated in hundreds sections from each sample at 48h, 9 and 21d. At 48h, the mean frequency of detecting one NP inside a cell section was around 15%, while at 9d it increased to 50-70%, with more NPs in each cell section. In general, the initial portion of the midgut had a higher amount of NPs and ingested materials (algae and yeast), if compared to the final portion. In 21d samples no differences have been observed in comparison to those from 9d.

The increase in the number of the observed NPs from 48h to 9d samples indicated the persistence of at least a good proportion of NPs for more than 48h, while the similar pattern of NPs occurrence in 9 and 21d samples suggested that NPs persistence did not exceed 9d.

Even at 48h but, more frequently, starting by 9d, NPs were observed: *i*) among and inside microvilli (Fig. 4A, B); *ii*) near the upper cell membrane; *iii*) inside the cytoplasm, either bound to the cytoplasmic side of the plasmatic membrane or as free NPs (Fig. 4C, D); *iv*) into mitochondria (Fig. 4E); *v*) in the paracellular space (Fig. 4C); *vi*) near the nuclear envelope (Fig. 4F), and inside the nucleus; *vii*) at the basement membrane level (Fig. 4G); *viii*) in the gut muscolaris and *ix*) in the eggs (Fig. 4H). The zinc composition of these NPs was confirmed by ESI analyses and some example was reported in Figure 5.

Looking at the cell morphology, the only difference detected between exposed and control samples, was the mitochondrial structure, which in samples at 9 and 21d appeared to be affected by NP exposure. Several mitochondria in all samples from these groups showed a disorganization of their cristae, with the presence of empty spaces. In some cases, both the inner and the outer mitochondrial membranes appeared lysed, as the last step of mitochondrial degeneration (Fig. 4D-E).

Differently from ZnO NPs exposure, no damage to mitochondria has been observed in $ZnSO_4$ samples (Fig. 6). On the contrary, a number of empty vacuoles with disorganised membranes have been detected (Fig. 6B). These figures were very similar to the autophagy vacuoles observed by (Santo et al., 2014) after exposure to high concentrations of the same compounds, even if in the present paper they were reduced in size and less frequent.

The potential Zn exposure coming from the internalization on NPs into gut cells can be calculated starting from the average number of NPs recorded into cells, their dimension and thus their volume and mass, in relation to the cell volume. Considering that a gut epithelial cell has a width and a thickness of about 8 µm and a height of 15-20 µm, the cell volume is 1120 μm^3 (8*8*17.5 µm). Because of a section for TEM analysis has a thickness of 60/70nm, the volume observed for each TEM section is near 1/130 of the total cell volume. From this, a mean number of 20 NPs/cell is derived (NPs had a frequency/probability in each section of 15%). Considering that the mean NP diameter is 20 nm (Santo et al., 2014), 20 NPs/cell have a volume of 8.4×10^{-5} μm^3, which corresponds to a weight of 47×10^{-5} pg (ZnO density = 5.61 pg/μm^3). In a cell volume of 1120 μm^3 the NP concentration becomes 0.042×10^{-5} pg/μm^3. This NP concentration corresponds to a potential release of zinc ion of 0.35 mg Zn/L. Obviously, NPs observed at TEM were not dissolved, but these calculations are

proposed in order to demonstrate that the dissolution of 20 NPs would be able to cause a quite high intra-cellular Zinc concentration. It is interesting noting that this concentration is similar to that of the soluble salt in the exposure media (0.3 mg Zn/L), which is unable to cause swelling of mitochondria. ZnO NPs did not cause this effect at 48h, but later when the NP number increased (9-21d) this happened. Considering that at 9 and 21d, NPs were much more frequent, the potential Zn concentration inside cells could be even higher.

4. Discussion

This work aimed to evaluate the chronic effects of low concentrations of ZnO NPs in comparison to the soluble Zinc, $ZnSO_4$. So far, three papers have studied the chronic toxicity of ZnO NPs on *D. magna* (Adam et al., 2014; Lopes et al., 2014; Zhao et al., 2012), but none has compared the chronic effects of ZnO NPs and soluble zinc by a morphological approach. Advance microscopic techniques have been here applied in order to detect and visualize the possible NPs internalization without huge contaminations, which are typical of acute toxicity exposures. Moreover, such an approach was also used to compare the effects of NPs and soluble salt on young and adults, for a better understanding of the toxicity mechanism of nanoZnO. Thus, the experimental plan of the present paper was specifically performed to obtain samples for the microscopic analyses, and not to gain those ecotoxicological parameters, such as NOEC, LOEC or EC_{50}, which have already been determined for *D. magna* and available in literature.

4.1. Life cycle parameters: comparison between nanoparticles vs. soluble Zn

Nominal concentrations for both $ZnSO_4$ and ZnO (0.1 and 0.3 mg Zn/L) were selected near and slightly above the EC_{50} values for chronic toxicity of these compounds on *D. magna*, as reported by (Adam et al., 2014): EC_{50} of 0.11 and 0.082 mg Zn /L for ZnO NPs and $ZnCl_2$, respectively. These concentrations are more realistic than those of acute toxicity, even if they are still far from the environmental concentrations given for ZnO NPs in natural waters, and which stay in the order of ng/L (Gottschalk et al., 2009). During exposure, the analytically-determined median concentrations of soluble Zn were lower than nominal ones, especially for the nanoparticulate form (<0.0084 and 0.059

mg Zn/L for nanoZnO at 0.1 and 0.3 mg Zn/L, respectively). Measured median concentrations of Zn ions for the soluble form ($ZnSO_4$) were at least three times higher (0.022 and 0.16 mg Zn/L at 0.1 and 0.3 mg Zn/L, respectively). Therefore, if toxic effects would come from soluble ions in the exposure medium, they should be greater for $ZnSO_4$ than for nanoZnO. Our data supported the hypothesis of a specific toxicity coming from the nanoparticulate form (ingestion of NPs and later events).

Looking at the toxicity levels of the to forms of Zn, the reproduction inhibition observed for both compounds (around 0.1 mg Zn/L) well agreed with results from (Adam et al., 2014) and (Lopes et al., 2014), while the range of chronic toxicity reported by (Zhao et al., 2012) was much lower than that observed in the present study.

The novelty of this work was the study of the recovery phase, after exposure. Detoxification and full-reproduction recovery were quite different among treatments, giving in one case a total reproduction even higher than that observed in control (exposure to nano ZnO at the lowest concentration). In this case, the higher reproduction potential was achieved by a positive effect on longevity. Interestingly, we observed at 21d an evident reduction of adult size only in samples exposed to ZnO NPs. Adam and colleagues too (Adam et al., 2014), observed a higher reduction in size in samples exposed to ZnO NPs (reduction of 12% in relation to control) *versus* those exposed to $ZnCl_2$ (2%). Basing on these evidences, we hypothesized that size reduction, specifically induced by the nanoparticulate form, was due to a slackening in the growth rate, which indirectly determined a higher longevity, once exposure was suspended. After a detoxification phase (first period after exposure), the reproductive potential was fully recovered, and the higher longevity (64 days *vs.* 57 of control) allowed adults to have a higher number of broads (18.2 *vs.* 15.2 in control), determining a total reproduction even higher than that registered in control (437 live neonates per female *vs.* 389 in control).

In literature, the comparison between soluble and nanoZn toxicity was exclusively studied by exposure trials; on the contrary our experiments, introducing the recovery phase, revealed important differences on the toxicity of the two form of Zn, even on life traits: nano ZnO showed a higher effect on reproduction (maximal inhibition during exposure), while soluble Zn specifically acted on longevity (reducing longevity at both concentrations). The explanation of this may derive by the interpretation of the mechanism of action of these two forms of Zn. First at all, it must be consider the role of Zn ions, which are also present after addition of nanoZnO. In literature, the role of zinc ions in ZnO NPs toxicity is still a very debated point. Several papers reported that ZnO NPs toxicity was due not only to the

solubilized ions, whose effects were different from those due to NPs (Bai et al., 2010; Hao et al., 2013; Poynton et al., 2011; Xiao et al., 2015); others strongly suggested that ZnO NPs toxicity was caused solely by them (Adam et al., 2014; Adam et al., 2015; Heinlaan et al., 2008). The relative toxicity of zinc ions directly released from ZnO NPs was recently studied by Xiao and co-workers (Xiao et al., 2015) who concluded that only 30% of the acute toxicity of ZnO NPs was due to released ions. The same authors reported that the role of dissolved ions may be different depending on concentration: at high concentrations (acute toxicity range) particles rather than Zn ions were the major source of toxicity, while at low concentrations (chronic range) the dissolved ions could be predominant. Bacchetta et al. (2016), by the same morfological approach used in this paper, concluded that the nano ZnO toxicity (at high concentrations) was mainly due to Zn ions, released inside cells by internalized NPs. A crucial point for establishing the role of solubilised ions in the ZnO NPs toxicity is the amount and velocity of ZnO NPs solubilisation. If the solubilisation is fast and almost complete, the possibility of a specific toxicity due to NPs become improbable, while if NPs persist longer, the possibility of specific effects of NPs is higher, and the toxicity can be either due to NPs themselves or to the *in-situ* solubilised ions. Unfortunately, solubilisation of ZnO NPs is far from being completely understood because it is greatly affected by many variables, such as coating, size and concentration, as well as by the medium characteristics such as pH and ionic strength. Adam and colleagues (Adam et al., 2014) reported that at low concentrations, namely in the range of the chronic toxicity, most of the ZnO NPs, even if aggregated, dissolved within 48h (average of 90.9 ± 2.5%), and according to (Xiao et al., 2015), they additionally showed that the dissolution was quite rapid (60% in 1-2h). At higher concentration ranges, ZnO NP solubility seemed to behave differently, with levels of solubilisation definitively lower and in the range of 4-18% (Poynton et al., 2011; Santo et al., 2014; Wang et al., 2009). According to the literature, the amount and proportion of solubilized ions in the test medium change greatly depending on the test conditions. The final concentration in the medium should be theoretically near the ZnO equilibrium solubility, thus the amount of the ZnO NPs solubilized can vary dramatically: from irrelevant fractions, when exposure concentrations are much above the equilibrium solubility, to nearly the whole amount, when exposure concentrations approach the maximum solubility. Our analytical results showed that, even at the lowest concentrations (0.1 mg Zn/L), the solubilized ions were limited to a fraction (<10% of total amount of Zn). In these conditions, ZnO NP can enter the digestive tract of *D. magna* and can be internalized in tissues and cells.

Differently from the soluble form, ZnO NPs have the specific role in physically carrying consistent Zinc amount into the organism, which in turn can locally increase ions concentration by intra-cellular solubilisation (Bacchetta et al., 2016). As discussed in the next paragraph, we hypothesized that the amount of Zn ions carried inside tissues and cells differed between the two chemicals, the nanoparticulate form being able to accumulate high intracellular Zn ions concentration by a secondary ions release subsequent to NP internalization.

Another interesting difference between NP and soluble Zn toxicity deals with the number of immobilized/dead daphnids observed in the nanoZnO and $ZnSO_4$ exposed groups and the time at which these specimens have been detected (end of exposure and immediately after it). These findings supported the conclusion that the effects on daphnids were not caused by a direct toxicity coming from the exposure media, but by an indirect toxicity coming from the mothers. In the first case in fact, daphnid immobilisation should have happened during the whole exposure phase, and should have stopped immediately after it. The finding that immobile samples have been mainly observed in the offspring of nanoZnO exposed groups and only at the end of the exposure period as well as in the first detoxification phase, supported the hypothesis that such an effect was mediated from mothers and was determined by the accumulation of NPs during exposures. This explanation was also supported by the detection, confirmed by ESI analysis, of many NPs within the eggs (Fig. 4H). Indeed, many nanomaterials, such as Au, TiO_2, SiO_2, polystyrene, quantum dots and carbon NPs, could penetrate the placental barrier (Chu et al., 2010; Sun et al., 2013), and some studies reported that e.g. TiO_2 NPs could cross even the blood–brain barrier (Wang et al., 2008). In this light, our finding is not surprising, even if never documented or reported before in *Daphnia* sp. Independently where these NPs have come from, and how they have reached the ovary, the risk associated to maternal exposure in offspring is clear. Takeda and co-workers (Takeda et al., 2009) demonstrated that TiO_2 NPs could be transferred from mother to offspring, damaging their reproductive and nervous systems. Also ZnO NPs have been reported to accumulate in mammary tissue of dams, as well as in kidney and liver of pups (Jo et al., 2013). These authors hypothesized that trans-placental and breastfeeding transport of ZnO nanomaterial actively occurred between pregnant mother and pups and concluded that even if fertility and mating parameters were unaffected by nanoZnO treatment, dams exposed to NPs before pregnancy and during gestation and lactation led to clear indications of developmental toxicity in the offspring (Jo et al., 2013). Of course multi-generation investigations are needed to fully understand the

risk associated to maternal exposure to NPs, but from the increasing number of paper on the topic it is clear that the interest of the scientific community towards this issue is far from being completely satisfied.

4.2. Microscopic analyses: comparison between nanoparticles vs. soluble Zn

Histological analyses didn't reveal any differences between the two compounds or between them and the controls, but images from ultrathin sections showed interesting discrepancies: first of all, the finding of ZnO NPs inside cells. Given the feeding behaviour of the species, the probability to find NPs in the digestive tract was high, but the possibility to detect them into cells was quite faint, considering the low level of exposure and the high solubility of ZnO NPs at low concentrations, as suggested by some authors (Adam et al., 2014). The finding of NPs inside different cell compartments of the digestive tract, and even outside it (presence confirmed by ESI analyses) was a key point for interpreting toxicity events, because it demonstrated that at least some NPs were able to be internalized in the cells of different tissues and to persist there in the nanoparticulate form. According to the findings of several authors (Bacchetta et al., 2012; Frohlich and Roblegg, 2012; Verma et al., 2008), the recent work of Santo and colleagues (Santo et al., 2014) described two possible internalization pathways: *i*) crossing through the cell membrane without disruption, mainly via the microvilli, and *ii*) following the endocytic pathway. Uptake by the microvilli was already reported also by (Harush-Frenkel et al., 2008) and by (Lovern et al., 2008) *in vitro* and *in vivo*, as well as the translocation of NPs outside the epithelial barrier (Bacchetta et al., 2012; Santo et al., 2014), but in all these cases the concentrations of ZnO NPs were high. The presence of NPs among and inside the microvilli (Fig. 4A-B) as well as their detection in the cytoplasm and paracellular spaces (Fig. 4B-D), confirmed the aforementioned entry routes and showed for the first time that also at low concentrations ZnO NPs can be internalized by enterocytes and can pass the epithelial barrier reaching other body districts.

The entry of NPs into cells gave an additional evidence of a possible specific toxicity due to the nanoparticulate form, and ultrastructural analyses of the midgut enterocytes supported once more this hypothesis. Mitochondria from samples exposed to ZnO NPs showed several damages, while those from $ZnSO_4$ did not. Many authors reported that mitochondria represented target organelles for ZnO NPs: Santo and colleagues (Santo et al., 2014) observed swollen mitochondria in the cytoplasm of the

digestive cells of *D. magna* exposed to nanoZnO identical to those observed here (Fig. 7A-B). According to other authors (Pi et al., 2013; Poynton et al., 2011; Zhu et al., 2009), they hypothesized that NPs induced mitochondrial damage via oxidative stress. Also Wiseman reported that ZnO NPs exposure led to mitochondria damage through ROS generation (Wiseman et al., 2007), and Xia (Xia et al., 2008) reported that metal oxide NPs, internalized into mitochondria, were able to produce locally soluble ions, which in turn induced the disruption of the organelles and triggered ROS generation. The same mechanism was demonstrated in the enterocytes of the amphibian *Xenopus laevis* exposed to ZnO NPs (Bacchetta et al., 2014), as well as in isolated rat liver mitochondria exposed to the same NPs (Li et al., 2003). However, the effects on mitochondria via oxidative stress caused by ROS production seemed to be a well-established toxic mechanism linked not only to ZnO NPs exposure, but also to soluble zinc (Cheng et al., 2010). Indeed, degeneration of mitochondria can be the common effect of ZnO NPs and $ZnSO_4$, (Bacchetta et al., 2016) but as reported above, at low concentrations damages to mitochondria were observed only after ZnO NPs exposure, and not after $ZnSO_4$ one. We believed that at low levels of exposure, only ZnO NPs were able to produce a zinc ions concentration sufficient to trigger the mitochondrial degeneration process. It is interesting noting that this effect was observed only at 9 and 21d, when evidences of NPs accumulation into epithelial cells were obtained. Adam et al. (2014) reported that the amount of Zn accumulated in organisms from NP exposure was similar to that coming from the exposure to the same concentration of soluble Zn (Zn ions from $ZnCl_2$), while Xiao et al. (2015) showed that the amount of Zn in organisms from NP exposure was higher than that coming from ions solubilised in the test medium from the corresponding ZnO NP concentration. These studies, apparently in contrast each other, actually tested different hypotheses, but they were unable to verify the effective accumulation of NPs inside the organism, because they measured total Zn concentration (sum of NPs and ions). Our work demonstrated that NP internalisation has already occurred at 48h and that NP accumulation continued at least until 9d. After this time a sort of plateau was reached in the NPs detection frequencies inside epithelial cells. We hypothesized that this NPs accumulation was able to produce a Zn ion concentration sufficient to produce the observed effects on mitochondria by day 9. According to this hypothesis, our $ZnSO_4$ exposures were unable to produce such an effect, while higher did. A very recent research (Bacchetta et al., 2016) reported that high concentrations of $ZnSO_4$ caused not only swollen mitochondria, but also the appearance of degenerative figures in the cytoplasm of the digestive cells, such as autophagy

vacuoles. In the present paper, these last figures have been observed in samples exposed to low $ZnSO_4$ concentrations (Fig. 7C), and were morphologically identical to those observed after high $ZnSO_4$ exposure, even if reduced in size and frequency (Fig. 7D). These figures are linked to cellular aging phenomena, as well documented in literature (Lipetz and Cristofalo, 1972). This last finding, extrapolated to the individual level, accords with the observed effect on longevity, which appeared to be specific of $ZnSO_4$ exposure.

5. Conclusions

The present work studied the chronic effects of ZnO NPs and $ZnSO_4$ exposure on *D. magna* also beyond the standard 21-day-exposure time and throughout the whole life cycle. TEM analyses demonstrated that at low concentrations insolubilized NPs did exist inside the gut, the epithelial cells and even the tissues beyond the epithelial barrier. NPs number increased from 48h until 9d, demonstrating the accumulation and persistence of NPs into *D. magna* tissues. Between 9 and 21d, NPs number did not increase, likely depending from two processes: *i)* the solubilisation of NPs inside cells, determining citotoxicity; *ii)* translocation to other body districts, with possible effects outside the midgut. Many NPs were observed in the ovary within eggs and, besides their fate has not been investigated further, a high number of immobilized daphnids were observed only after ZnO NPs exposure, and only at the end of the exposure period (21d). This suggested that effects on daphnids were caused by the chronic accumulation of NPs in mothers with a translocation to reproductive cells (transfer of the contamination from the mothers to the offspring). Such an issue is worthy of more detailed studies, and raises concerns about the risk associated to an uncontrolled use of NPs.
Both ultrastructural observations and macroscopic effects on fitness during the whole life cycle indicated different toxicity effects between the two compounds, at least at low concentrations. We believed that ZnO NPs ingested by *D. magna* were able to carry an amount of zinc higher than that provided by the soluble form, and sufficient to cause a direct damage to mitochondria. This would be responsible for low energy availability at body level and for the consequent reduction of growth and reproduction. Differently from NPs, $ZnSO_4$ exposed samples did not show any evident growth reduction, but a lower reproduction and a reduced longevity. Our morphological analyses, which revealed the presence of figures linked to the physiological process of cellular aging, suggested that

the observed reduction of longevity could be related to an accelerated cellular aging phenomenon. Under this condition, cell efficiency may be reduced (lower reproduction than the control) and the life cycle shortened (lower longevity than the control). Thus, at low concentrations ZnO NPs determined effects different from those due to the same amount of soluble zinc, macroscopically on the life cycle parameters and microscopically on the epithelial cell ultrastructure. We believe that these differences derived from the ability of NPs of carrying into specific cells and tissues a higher amount of Zn than the corresponding soluble form, by the combination of an efficient NP internalisation and accumulation phenomena. These considerations led to the conclusion that Zn ions still play a key role on ZnO cytotoxicity, but that NPs are able to cause specific toxic effects because of their capacity of efficient carriers of soluble ions into cells.

Acknowledgements

Authors would like to thank Dr Maria Carla Panzeri and Dr Paola Podini for their technical help and for the facilities they kindly provided. Authors are also grateful to B.A. Maria Luisa Bonicalzi for help maintaining daphnid cultures, and to three anonymous reviewers for their constructive comments, which helped to improve the manuscript.

References

Adam, N., et al., 2014. The chronic toxicity of ZnO nanoparticles and $ZnCl_2$ to *Daphnia magna* and the use of different methods to assess nanoparticle aggregation and dissolution. Nanotoxicology. 8**,** 709-717.

Adam, N., et al., 2015. Gene transcription patterns and energy reserves in *Daphnia magna* show no nanoparticle specific toxicity when exposed to ZnO and CuO nanoparticles. Environmental Research. 138**,** 82-92.

Aruoja, V., et al., 2009. Toxicity of nanoparticles of CuO, ZnO and TiO_2 to microalgae *Pseudokirchneriella subcapitata*. Science of the Total Environment. 407**,** 1461-1468.

Bacchetta, R., et al., 2016. Role of soluble zinc in ZnO nanoparticle cytotoxicity in *Daphnia magna*: A morphological approach. Environmental Research. 148**,** 376-385.

Bacchetta, R., et al., 2014. Evidence and uptake routes for Zinc oxide nanoparticles through the gastrointestinal barrier in *Xenopus laevis*. Nanotoxicology. 8**,** 728-744.

Bacchetta, R., et al., 2012. Nano-sized CuO, TiO_2 and ZnO affect *Xenopus laevis* development. Nanotoxicology. 6**,** 381-398.

Bai, W., et al., 2010. Toxicity of zinc oxide nanoparticles to zebrafish embryo: a physicochemical study of toxicity mechanism. Journal of Nanoparticle Research. 12**,** 1645-1654.

Chang, N., Jenkins, D. G., 2000. Plastid endosymbionts in the freshwater crustacean *Daphnia obtusa*. Journal of Crustacean Biology. 20**,** 231-238.

Cheng, W. Y., et al., 2010. An Integrated Imaging Approach to the Study of Oxidative Stress Generation by Mitochondrial Dysfunction in Living Cells. Environmental Health Perspectives. 118**,** 902-908.

Chu, M., et al., 2010. Transfer of quantum dots from pregnant mice to pups across the placental barrier. Small. 6**,** 670-678.

David, C. A., et al., 2012. Dissolution Kinetics and Solubility of ZnO Nanoparticles Followed by AGNES. Journal of Physical Chemistry C. 116**,** 11758-11767.

Elder, A., et al., 2009. Physicochemical factors that affect metal and metal oxide nanoparticle passage across epithelial barriers. Wiley Interdisciplinary Reviews-Nanomedicine and Nanobiotechnology. 1**,** 434-450.

Farre, M., et al., 2009. Ecotoxicity and analysis of nanomaterials in the aquatic environment. Analytical and Bioanalytical Chemistry. 393**,** 81-95.

Franklin, N. M., et al., 2007. Comparative toxicity of nanoparticulate ZnO, bulk ZnO, and $ZnCl_2$ to a freshwater microalga (*Pseudokirchneriella subcapitata*): The importance of particle solubility. Environmental Science & Technology. 41**,** 8484-8490.

Frey, D. G., 1982. Contrasting strategies of gamogenesis in Northern and Southern populations of Cladocera Ecology. 63**,** 223-241.

Frohlich, E., Roblegg, E., 2012. Models for oral uptake of nanoparticles in consumer products. Toxicology. 291**,** 10-17.

Gottschalk, F., et al., 2009. Modeled Environmental Concentrations of Engineered Nanomaterials (TiO_2, ZnO, Ag, CNT, Fullerenes) for Different Regions. Environmental Science & Technology. 43**,** 9216-9222.

Hao, L. H., et al., 2013. Bioaccumulation and sub-acute toxicity of zinc oxide nanoparticles in juvenile carp (*Cyprinus carpio*): A comparative study with its bulk counterparts. Ecotoxicology and Environmental Safety. 91**,** 52-60.

Harush-Frenkel, O., et al., 2008. Surface charge of nanoparticles determines their endocytic and transcytotic pathway in polarized MDCK cells. Biomacromolecules. 9**,** 435-443.

Heinlaan, M., et al., 2008. Toxicity of nanosized and bulk ZnO, CuO and TiO_2 to bacteria *Vibrio fischeri* and crustaceans *Daphnia magna* and *Thamnocephalus platyurus*. Chemosphere. 71**,** 1308-1316.

Jo, E., et al., 2013. Exposure to zinc oxide nanoparticles affects reproductive development and biodistribution in offspring rats. Journal of Toxicological Sciences. 38**,** 525-530.

Kahru, A., Dubourguier, H. C., 2010. From ecotoxicology to nanoecotoxicology. Toxicology. 269**,** 105-119.

Li, N., et al., 2003. Ultrafine particulate pollutants induce oxidative stress and mitochondrial damage. Environmental Health Perspectives. 111**,** 455-460.

Lipetz, J., Cristofalo, V. J., 1972. Ultrastructural changes accompanying the aging of human diploid cells in culture. J Ultrastruct Res. 39**,** 43-56.

Lopes, S., et al., 2014. Zinc Oxide Nanoparticles Toxicity to *Daphnia Magna*: Size-Dependent Effects and Dissolution. Environmental Toxicology and Chemistry. 33**,** 190-198.

Lovern, S. B., et al., 2008. Electron microscopy of gold nanoparticle intake in the gut of *Daphnia magna*. Nanotoxicology. 2**,** 43-48.

Mayhew, T. M., et al., 2009. A review of recent methods for efficiently quantifying immunogold and other nanoparticles using TEM sections through cells, tissues and organs. Annals of Anatomy-Anatomischer Anzeiger. 191**,** 153-170.

OECD, 2012. Test No. 211: *Daphnia magna* Reproduction Test. OECD Publishing.

Pi, J., et al., 2013. Pathway of cytotoxicity induced by folic acid modified selenium nanoparticles in MCF-7 cells. Applied Microbiology and Biotechnology. 97**,** 1051-1062.

Poynton, H. C., et al., 2011. Differential Gene Expression in *Daphnia magna* Suggests Distinct Modes of Action and Bioavailability for ZnO Nanoparticles and Zn Ions. Environmental Science & Technology. 45**,** 762-768.

Quaglia, A., et al., 1976. Studies on the intestine of Daphnidae (Crustacea, Cladocera) ultrastructure of the midgut of *Daphnia magna* and *Daphnia obtusa*. Journal of Morphology. 150**,** 711-725.

Santo, N., et al., 2014. Toxic effects and ultrastructural damages to *Daphnia magna* of two differently sized ZnO nanoparticles: Does size matter? Water Research. 53**,** 339-350.

Schultz, T. W., Kennedy, J. R., 1976. The fine structure of the digestive system of *Daphnia pulex* (Crustacea: Cladocera). Tissue Cell. 8**,** 479-490.

Sun, J., et al., 2013. Effects of nanotoxicity on female reproductivity and fetal development in animal models. International Journal of Molecular Sciences. 14**,** 9319-9337.

Takeda, K., et al., 2009. Nanoparticles Transferred from Pregnant Mice to Their Offspring Can Damage the Genital and Cranial Nerve Systems. Journal of Health Science. 55**,** 95-102.

Vaseem, M., et al., ZnO Nanoparticles: Growth, Properties, and Aplications. In: A. Umar, Y.-B. Hahn, Eds.), Metal Oxide Nanostructures and their Applications. American Scientific Publishers, Los Angeles, USA, 2010, pp. 1-36.

Verma, A., et al., 2008. Surface-structure-regulated cell-membrane penetration by monolayer-protected nanoparticles. Nature Materials. 7**,** 588-595.

Wang, H. H., et al., 2009. Toxicity of nanoparticulate and bulk ZnO, Al_2O_3 and TiO_2 to the nematode *Caenorhabditis elegans*. Environmental Pollution. 157**,** 1171-1177.

Wang, J. X., et al., 2008. Time-dependent translocation and potential impairment on central nervous system by intranasally instilled TiO_2 nanoparticles. Toxicology. 254**,** 82-90.

Wiench, K., et al., 2009. Acute and chronic effects of nano- and non-nano-scale TiO_2 and ZnO particles on mobility and reproduction of the freshwater invertebrate *Daphnia magna*. Chemosphere. 76**,** 1356-1365.

Wiseman, D. A., et al., 2007. Alterations in zinc homeostasis underlie endothelial cell death induced by oxidative stress from acute exposure to hydrogen peroxide. American Journal of Physiology-Lung Cellular and Molecular Physiology. 292**,** L165-L177.

Xia, T., et al., 2008. Comparison of the Mechanism of Toxicity of Zinc Oxide and Cerium Oxide Nanoparticles Based on Dissolution and Oxidative Stress Properties. Acs Nano. 2**,** 2121-2134.

Xiao, Y. L., et al., 2015. Toxicity and Accumulation of Cu and ZnO Nanoparticles in *Daphnia magna*. Environmental Science & Technology. 49**,** 4657-4664.

Zhao, H.-z., et al., 2012. Toxicity of nanoscale CuO and ZnO to *Daphnia magna*. Chem. Res. Chinese Universities. 28**,** 209-213.

Zhu, X. S., et al., 2009. The impact of ZnO nanoparticle aggregates on the embryonic development of zebrafish (*Danio rerio*). Nanotechnology. 20**,** 195103.

Chronic toxicity effects of $ZnSO_4$ and ZnO nanoparticles in *Daphnia magna*

Renato Bacchetta [a,*], Nadia Santo [a], Marcello Marelli [b], Greta Nosengo [a], Paolo Tremolada [a]

[a] Department of Life Sciences, Università degli Studi di Milano, Via G. Celoria, 26, I-20133 Milan, Italy

[b] CNR-ISTM - Istituto di Scienze e Tecnologie Molecolari, Via C. Golgi, 19, I-20133 Milan, Italy

* *Corresponding author*.

Renato Bacchetta

Tel: +39 02 503 14783; fax: +39 02 503 14781

E-mail address: renato.bacchetta@unimi.it

Department of Life Sciences

Università degli Studi di Milano

Via G. Celoria, 26

I-20133 Milan, Italy

Abstract

The chronic toxicity of $ZnSO_4$ and ZnO nanoparticles has been studied in *Daphnia magna* also considering the life cycle parameters beyond the standard 21-day exposure time. Specimens have been individually followed until the natural end of their life, and some of them sampled for microscopic analyses at 48 hours, 9 and 21 days. Despite the low level of exposure (0.3 mg Zn/L), ultrastructural analyses of the midgut epithelial cells revealed efficient internalization of nanoparticles between 48h and 9d, and translocation to other tissues as well. At 21d, the most affected fields have been recorded for both compounds; in particular samples exposed to ZnO nanoparticles showed swelling of mitochondria, while those exposed to $ZnSO_4$ had a great number of autophagy vacuoles. The life cycle parameters resulted altered as well, with a significant inhibition of reproduction in both groups, when compared to controls. After the 21-day exposure, some interesting results were obtained: animals, previously exposed to nanoZnO at low concentrations, showed a complete recovery of the full reproduction potential, while those previously exposed to $ZnSO_4$ presented a dose-dependent and compound-specific reduction in lifespan. Based on the results from the present research and the effects of the same chemicals at higher doses, it can be concluded that the soluble form plays a key role in ZnO nanoparticle cytotoxicity, and that the nanoparticulate form is able to locally increase the amount of Zn inside the cell, even within the ovary. It's worth noting that ZnO nanoparticles have been internalized despite the very low concentration used: this raises concern about the possible environmental implications which may derive from their use, and which in turn must be carefully considered.

Keywords: Toxicity; Ionic Zinc; Zinc oxide; Daphnia magna; TEM.

1. Introduction

Toxicological properties of nanoparticles (NPs) are currently under investigation because of their large applications in industry and common-use products. Due to their well-known chemico-physical characteristics (Vaseem et al., 2010), ZnO NPs are among the most used NPs and consequently subjected to be dispersed in the environment (Kahru and Dubourguier, 2010). In the last years, the ecotoxicity of NPs and in particular the effects of ZnO on organisms have been largely studied (Farre et al., 2009). Toxicological data of ZnO NPs revealed a wide range of sensitivity among species: algae were the most sensible with EC_{50} values around 0.05 mg Zn/L (Aruoja et al., 2009; Franklin et al., 2007), while bacteria and nematoda showed EC_{50} values as high as 800 mg Zn/L (Heinlaan et al., 2008; Wang et al., 2009). Protozoa, crustacean and fish showed intermediate EC_{50s}, ranging from less than 1 mg Zn/L (Wiench et al., 2009) up to 18 mg Zn/L (Bai et al., 2010). Nevertheless, the question on the relative contribution to toxicity of the dissolved ions, as well as their action mechanisms in NP cytotoxicity still remained open. Recent studies have begun considering the different contribution to the overall toxicity of the different forms in metal oxide NPs; it is well known in fact that the overall toxicity of a given NP (Tox_{tot}) is the result of the toxicity of the NP itself (Tox_{part}) and that from the solubilized ion (Tox_{ion}). (Xiao et al., 2015) measured the acute toxicity of ZnO NPs in *Daphnia magna*, considering the contribution of the dissolved ions (Tox_{ion}) after centrifugation and filtration, and concluded that most of the toxicity was due to NPs, being the Tox_{ion} contribution around 31%. The same authors showed that the internal concentration of Zn was proportional to the concentration of ZnO NPs administered to daphnids. Moreover, they observed that at high NP concentrations the Tox_{part} played a dominant role, while at low NP concentrations, Tox_{ion} overshadowed the effects of NPs. Several authors affirmed that in the exposure medium a large fraction of NPs rapidly dissolves (Adam et al., 2014; Xiao et al., 2015), while others, measuring very low levels of dissolved ions in the medium, concluded that the dissolution can happen, but mainly inside the cells after NP internalization (Santo et al., 2014). Discrepancies in the percentages of dissolved ion amounts are likely due to the NPs concentration relatively to the equilibrium solubility of ZnO NPs, which is at the mg/L level (David et al., 2012), and also to the combined effects exerted by NP characteristics (presence of coatings, particle size) and exposure medium (ionic strength and pH). Although reasons may be different, depending on NPs and experimental conditions, the majority of authors agree that ZnO NPs toxicity

can be largely attributed to the dissolved fraction, independently from where it happens: in the exposure medium or inside the cell (Adam et al., 2014; Adam et al., 2015; Heinlaan et al., 2008; Santo et al., 2014).

Contrary to acute toxicity, chronic toxicity of ZnO NPs is less studied and more realistic, since generally it happens below 1 mg/L. At low concentrations, the NP behavior can be different and primary internalization and toxicity mechanisms can be better studied with respect to acute toxicity. Only three studies have considered the chronic toxicity of ZnO NPs on *D. magna.* (Zhao et al., 2012) reported very low NOEC (no observed effect concentration) and LOEC (lowest observed effect concentration) values (0.0006 and 0.003 mg Zn/L, respectively), in comparison to the higher values found by (Adam et al., 2014) (0.058 and 0.131 mg Zn/L, respectively) and by (Lopes et al., 2014), who reported a LOEC value of 0.125 mg Zn/L. (Adam et al., 2014) obsereved similar chronic effects on growth, reproduction and accumulation for the ZnO nanoparticles ($EC_{10,\ 20,\ 50}$ of 0.030, 0.049, 0.112 mg Zn/l, respectively) and the $ZnCl_2$ ($EC_{10,\ 20,\ 50}$ of 0.014, 0.027, 0.082 mg Zn/l, respectively), while (Lopes et al., 2014), using differently sized ZnO NPs, showed higher effects for the smaller NPs, but similar effects between the NPs and the dissolved ions. Both these papers concluded that NPs toxicity on *D. magna* reproduction parameters was due to zinc ions.

In the present paper the chronic toxicity of ZnO NPs and that of the soluble zinc salt $ZnSO_4$ have been investigated on *D. magna* by ultrastructural analyses of the midgut cells, during the 21-day chronic test. In addition, the reproduction and life parameters have been recorded and analyzed also after the 21-day exposure, until the end of the whole life cycle (recovery phase). The main questions for the ultrastructural analyses were: *i)* do the internalizations of NPs happen also at low concentrations? and *ii)* does chronic toxicity, with its low level of exposure, cause morphological alterations as well? On the contrary, considering the life cycle assessment: *iii*) are there any differences among treatments? *iv*) are these differences, if any, also evident at the end of the recovery phase? and finally *v*) can the role of (Tox_{part}) and that of (Tox_{ion}) be determined by this double comparison (ultrastructural effects and life cycle behavior)?

2. Material and methods

2.1. Experimental plan

Chronic effects of ZnO NPs and soluble Zn salt, $ZnSO_4$, were analysed during the whole life cycle of *Daphnia magna*. The experimental plan consisted in an exposure phase of 21d, followed by a recovery phase, until the natural end of the life cycle of each animal (around 60d). Exposures were conducted with two concentrations: 0.1 and 0.3 mg Zn/L of nanoZnO and $ZnSO_4$ together with the controls, and samples were fixed for the analyses at three different times: 48h, 9 and 21d.

2.2. ZnO NPs and $ZnSO_4$

Zinc oxide NPs with an advertised particle diameter <50 nm, were purchased from Sigma-Aldrich (Milano, Italy; lot number #MKBD9623V). Stock and exposure suspensions were prepared according to the protocol for nanoparticle dispersions suggested by the PROSPEcT Project in accordance with the agreed OECD WPMN 'Guidance Manual for Sponsors of the OECD Sponsorship Programme for the Testing of Manufacture Nanomaterials'. Briefly, nanoZnO was weighted, initially dispersed in few drops of medium water, then in 20 mL. The obtained suspensions were sonicated for 30 second at 20 Khz ± 50 hz, then diluted, sonicated again at the same conditions and used to obtain the stock suspensions (50 and 150 mg Zn/L, respectively). These were always sonicated as above before use. The Zinc salt, $ZnSO_4$ anhydrous, was purchased from Carlo Erba (Carlo Erba Reagents, Milano, Italy). Two stock solutions of $ZnSO_4$ at a concentration of 50 and 150 mg Zn/L were prepared in deionized water.

2.3. NP characterization

The effective diameters of more than 500 NPs were randomly evaluated by Transmission Electron Microscopy (TEM) and their size distributions measured by the EsiVision software (Olympus, Germany). ZnO NPs were additionally analyzed for purity using a Zeiss LEO 1430 Scanning Electron Microscope (SEM), coupled with a Centaurus detector for energy dispersive X-ray spectroscopy analysis (EDX). Dynamic Light Scattering (DLS) was used to characterize the hydrodynamic behavior of the NPs and their extent of aggregation in the same water used for the animal exposure tests, and

the Z-potential was registered with a Malvern Nanosizer ZS, (Malvern, UK). Data about the NP characterization are available in (Santo et al., 2014).

2.4. Test species

The freshwater crustacean *Daphnia magna* Straus, originally obtained from the Istituto Superiore di Sanità (ISS, Roma, Italy) and maintained by the authors at the University of Milan, was used as test species. Specimens (30 ind/L) were cultured in a commercial mineral water (San Benedetto®, whose chemico-physical parameters were: conductivity 415 µS cm^{-1} at 20°C, pH 7.42, 301 mg/L HCO_3^-, 48.6 mg/L Ca^{2+}, 28.2 mg/L Mg^{2+}). Cultured daphnids were fed a suspension of the unicellular green alga *Pseudokirchneriella subcapitata* (0- to 8-day-old daphnids: 8 x 10^6 cells ind^{-1} day^{-1} and from 8-day-old daphnids: 16 x 10^6 cells ind^{-1} day^{-1}) and the yeast *Saccharomyces cerevisiae* (15 x 10^6 cells mL^{-1}), three times a week. The culture medium was renewed and offspring discarded three times a week. The breeding cultures were renewed every 5/6 weeks and replaced with neonatal organisms. Daphnids from the fourth reproduction cycle were taken for culture renewal and for the exposure experiments. Culture and exposure solutions were maintained at 20.5 ± 0.5 °C under a 16 h light: 8 h dark photoperiod. According to Frey (Frey, 1982), the above conditions assure continuous amictic parthenogenetic reproduction in cultures. Algae were cultured in ISO 8692:1989 medium within a 2L flask at 20 ± 2°C under continuous light and shaken by bubbling air. Algae were harvested during their exponential growth and left in the dark at 4°C for sedimentation for 8 days. After supernatant elimination, cell density of the concentrated algal suspension was determined using a Burker counting chamber under a Zeiss light microscope.

2.5. Chronic toxicity test and recovery phase

The exposure phase was performed in agreement with the standard 21d chronic reproduction test (OECD, 2012). Stock solutions of $ZnSO_4$ and nanoZnO were freshly prepared before the experiments and used for the two exposure concentrations of 0.1 and 0.3 mg Zn/L, as described above. According to the OECD recommendations, Zinc ion concentrations in $ZnSO_4$ solutions and the amount of Zn solubilized from NPs in the nanoZnO suspensions were measured in duplicates by Inductively Coupled Plasma - Optical Emission Spectrometry, ICP-OES (Thermo Scientific iCAP6300 Duo, Waltham, MA, USA) after preparation, 24h later, and after 48h. Samples for the analytical

determination of Zinc concentration in $ZnSO_4$ groups were filtered with 0.2 μm Nalgene syringe filters with Teflon PTFE membranes (Thermo Fisher Scientific, Milano, Italy), acidified to 1% HNO_3 (≥ 69%, traceSELECT for trace analysis, FLUKA, Seelze, Germany) and maintained in the dark at 4°C. ICP-OES analyses were performed at three characteristic wavelengths for Zn (202.548, 206.200 and 213.856 nm) with very consistent results (mean RSD = 2.0 %). Quantifications were performed at 202.548 nm by a 5-points external calibration line (calibration range: from 0.05 to 0.5 mg Zn/L) with the bracketing method. Each determination was repeated 5 times (mean RSD = 0.47 %). The limit of detection was evaluated at 0.0084 mg Zn/L. Measured Zn concentrations in milliQ water, San Benedetto® mineral water (blank reference), and in control samples at 0, 24 and 48h were below this limit. Measured Zn concentrations in exposure media before the experiments were close to the nominal ones (mean difference in percentage = 6.8 %).

To estimate the possible contribution to toxicity of the zinc ions dissolved from ZnO NPs, ZnO suspensions were ultrafiltered using centrifuge tubes VIVASPIN 20 with a molecular weight cut off of 10 KDa (Sartorius Stedim Biotech GmbH, Goettingen, Germany) in a swing out Eppendorf 5804 R centrifuge (Eppendorf Italia, Milano, Italy) running at 4000 g for 15 min. Filtrates were acidified to 1% HNO_3 and stored at 4°C in dark.

For each treatment group, 15 or 20 replicates of 1 daphnid (<24h) were used. The exposures were conducted in glass beakers containing 50 mL of test medium. The number of replicates was higher than that required by the OECD protocol (n = 10), in order to guarantee a sufficient number of samples at the end of the 21d exposure time, considering those specimens to be fixed for the microscopic analyses at 48h, 9 and 21d. During the exposure phase, daphnids were transferred every 2 days to clean glass beakers filled with freshly prepared medium and fed with *P. subcapitata* and *S. cerevisiae* as indicated above.

At 21 days, the total number of living offspring and mothers were counted in order to match the OECD requirements. The following recovery phase started the 21st day and continued until the end of the life cycle for each animal. During the recovery phase no exposure to nanoZnO or $ZnSO_4$ was performed and specimens were fed as specified above.

During the exposure and recovery phases, all the experimental groups were maintained at 20.5 ± 0.5 °C under a 16 h light: 8h dark photoperiod and the number of living, immobile and dead offspring

were recorded daily. Animals unable to swim within 15 s of gentle agitation of the test container were considered immobile, while those whose heartbeats have stopped were considered dead.

2.6. Light and electron microscopy

Specimens for histological and ultrastructural analyses were randomly selected and fixed in a mixture of 2% paraformaldehyde and 2.5% glutaraldehyde in 0.1 M sodium cacodylate buffered solution at pH 7.4. After washes in the same buffer, daphnids were post-fixed in 1% OsO_4 for 1 h in dark condition, dehydrated in a graded ethanol series and finally in 100% propylene oxide. Infiltration was subsequently performed with propylene oxide and resin (Araldite-Epon) at volumetric proportions of 2:1 for 1.5 h and 1:1 overnight. Daphnids were then embedded in 100% pure resin for 5 h, and polymerization was performed at 60°C for 48h. Sectioning was performed using an Ultracut E microtome (Reichert, Austria): semithin sections of about 1µm were collected onto microscope slides and stained with 1% toluidine blue to select the region of interest. The histological analysis was performed on semithin sections of 0.5 µm from 5 specimens from each treatment group, control included. For the ultrastructural analysis, 15-20 ultrathin sections of about 60/70 nm from the midgut of each sample were collected on 600-mesh uncoated copper grids. Due to the very low level of exposure and in order to maximize the possibility of evidencing cellular damages in the samples, only the 0.3 mg Zn/L groups (nanoZnO and $ZnSO_4$) have been considered for the ultrastructural analyses and 3 daphnids at 48h, 4 at 9d and 5 at 21d from each experimental group, control included, have been processed for a total of 36 samples analyzed. All thin sections were not counterstained and observed with a Zeiss LEO 912ab Energy Filtering TEM operating at 120 kV. Digital images were acquired using a CCD-BM/1K system operating with the ESI vision software AnalySIS (Soft Imaging Systems, Muenster, Germany).

2.7. Data analyses and statistics

The following reproductive parameters were calculated during the exposure and recovery phases: total number of live offspring per female, total number of immobile/dead offspring per female, time to first broad per female and number of broads per female. From those parameters, mean broad size (mean number of offspring per broad) and mean time between broads were derived. In addition, the eventual early mortality during the experiment (those happened before the 50^{th} days) and the longevity

(days from birth for the animal died after the 50th day) was recorded. Reproductive endpoints among exposed and control specimens were compared in a one-way ANOVA with Bonferroni multiple comparison test and immobile offspring *vs.* control ratio was analysed by Mann-Whitney test. Survival probabilities were calculated according to the Kaplan-Meir method with Log-Rank statistic for testing exposure-control differences. Longevity in controls and treated groups was calculated by probit regression as time at which the 50% of cases died. 95% confidence intervals of mean longevity were reported too. All statistical analyses were performed with SPSS software ver. 15.0. Live offspring *vs.* control difference in percentage was calculated as the mean difference of the total live offspring in treated animals and the mean total live offspring in control, with respect to the mean total live offspring in control ± standard deviation. Immobile offspring *vs.* control ratio was calculated as the mean ratio of the total immobile offspring in treated animals and mean total immobile offspring in control ± standard deviation. Longevity *vs.* control difference in days was calculated as the mean difference of the mother longevity in treated animals and the mean mother longevity in control ± standard deviation.

3. Results

3.1. Exposure test and life cycle behaviour

D. magna life cycle was divided into two phases: an exposure phase (0-21 days), when treated groups were exposed to chemicals, and a recovery phase, from day 21 to death. Data were split into two different paragraphs corresponding to the two phases described above. Table 1 reported, for each phase and for the whole life cycle, the number of live and immobile/dead neonates per female, together with the lifespan of all samples. The complete set of parameters was listed in Tables S1 and S2, available in the online version of the paper. During the exposure, no mortality was registered among the mothers in control groups and a mean of 66 ± 10 and 70 ± 12 daphnids per *Daphnia* was recorded in the controls for 0.1 and 0.3 mg Zn/L respectively, thus matching the OECD conditions for the validity of the test. As required by the same guidelines, Zn concentrations (referring to the soluble fraction) were analytically measured in the test medium for both exposure and control batches at 1, 24 and 48 h. The first time (1 h) takes into account the lag time necessary for adding algae, yeast and the

test species before the water sampling for determination, and the last time (48 h) corresponds to the time for the renewal of solutions.

As already reported above, soluble Zinc concentrations in the exposure medium after $ZnSO_4$ addition were measured just before animal and food addition (time 0) and were very close to the nominal ones (mean difference of 6.8%). In about 1 h (first sampling after animal and food addition), Zinc concentrations dropped to 66 and 73% of the nominal ones for 0.1 and 0.3 mg Zn/L, respectively. This decrease was likely due to the adsorption by the test species, but mainly by algae and yeast, which had a high surface area in relation to their mass. These latter were likely the most responsible for the observed decrease, since in previous experiments with $ZnSO_4$, in which *D. magna* has been exposed without food sources, soluble Zn concentrations after 48 h from the chemical addition were near the 80% of the initial mass (Bacchetta et al., 2016). On the contrary, in the present conditions the decrease was evident, especially at the lowest concentration. In fact, the median measured concentrations during the renewal interval (0.022 and 0.16 mg Zn/L) were even lower than the half of the nominal concentrations (0.1 and 0.3 mg Zn/L, respectively). Because of this, the effects observed during exposure and recovery phases, must be related to measured concentrations and not to nominal ones. Anyway, for comparison porpoise with the other compound for which the soluble amount was not the only contamination source, nominal concentrations 0.1 and 0.3 mg Zn/L will be maintained in the text.

After nanoZnO addition, soluble zinc concentrations above LOD were registered only for the highest concentration (0.3 mg Zn/L), while they were below LOD (<0.0084 mg Zn/L which means <8.4% of the initial mass) for the lowest one (0.1 mg Zn/L). When concentrations were measured above LOD, a decreasing concentration trend between 1 and 48 h was observed and again, this was likely due to the absorption by organisms. The initial soluble fraction was 24% of the added nanoparticle mass and the final one was 9.4%, indicating that NPs were only partially solubilized. In previous experiments with the same nanoparticles, the amount of soluble Zinc released by NPs was only 2-5% of the initial Zn mass (Santo et al, 2014), and the soluble fraction remained quite constant during the period between renewals (48 h). Despite these discrepancies, the most important result from these analytical measurements was that most of the nanoZnO mass (around 80%) did not solubilize (at least outside organisms), remaining in the particulate form. This evidence was conformed visually, observing

deposition of ZnO NPs in the exposure beakers, and by microscopic analyses, by the observation of many NPs in the gut lumen and inside tissues (as described below).

3.1.1. Exposure phase (0-21 days)

At the lowest concentration, the total number of live offspring per female was significantly lower than in controls ($p=0.001$ and $p=0.011$ for nanoZnO and $ZnSO_4$, respectively), while no statistically significant differences were present between the two chemicals (Table 1). Also the mean brood size per female was lower in treated groups, but without significant differences in respect to control and between the two compounds (Table S1). Even though slightly retarded for both compounds, no statistically differences were observed in the time of the first brood and in the number of brood per female, which however resulted reduced mainly after nanoZnO exposure (Table S1).

At the highest concentration, the total number of live offspring per female was significantly lower than in controls ($p<0.001$ and significant differences between the two chemicals were present, Table 1). Mean brood size per female and the time to first broad were lower and retarded, respectively for both chemicals *vs*. controls, but with significant difference only for nanoZnO (Table S1). The maximal inhibition percentage was reached after 21 days (71 ± 5.2 % and 43 ± 9.5 % for nanoZnO and $ZnSO_4$, respectively) and, at the highest concentration, a high number of immobile/dead daphnids was observed only in the exposed groups, especially following nanoZnO exposure (Table 1). Interestingly, these specimens were mainly observed at the end of the exposure period and in the first days subsequent to the onset of the recovery phase. All reproduction parameters suggested that ZnO NPs had more adverse effects on *D. magna* reproduction than $ZnSO_4$, even if the concentration of soluble Zn in $ZnSO_4$ groups was near 3-fold higher than that measured in ZnO ones.

3.1.2. Recovery phase (21-end of the life cycle)

The recovery phase started from day 21, with the end of the exposure period, and aimed to assess the possible reversibility of the chronic toxicity. Figure 1 showed the survival probability curves of exposed and control groups. For both concentrations and compounds, longevity of exposed animals *vs.* control was significantly different at Log-Rank test ($p<0.001$).

During the recovery phase, reproduction parameters and longevity showed different results, depending on concentration and compound. Animal previously exposed to 0.1 mg Zn/L of nanoZnO

exhibited a significant higher number of live neonates per female than controls (Table 1). The longevity of the mothers was higher too, while time between brood and mean brood size did not differ from controls (Table S2), suggesting that the higher reproduction was due to the higher number of broods because of the longer life (mean number of broods per female was significantly higher than that of control, Table S2). An interesting observation, even if not quantitatively evaluated, concerned the body size of specimens at the beginning of the recovery phase. Samples exposed to $ZnSO_4$ did not show evident differences if compared to controls, while those exposed to nanoZnO were much smaller than the others. As stated above, this item was not supported by direct measurement; anyway this qualitative observation was confirmed by literature data, as reported later in the discussion.

Animals previously exposed to the lowest concentration of $ZnSO_4$ showed slightly lower longevity than controls (mean difference vs. control of -3.9 ± 4.0 days) and a reproduction not significantly different from controls (Table 1).

In synthesis, animals exposed to nanoZnO and $ZnSO_4$ at the lowest concentration exhibited similar effect during the exposure (partial inhibition of the reproduction efficiency), but later, during the recovery phase, they presented a very different behaviour. In fact, animals previously exposed to nanoZnO showed a higher reproduction than control because of a higher longevity, while animals previously exposed to $ZnSO_4$ presented almost the same reproduction efficiency than control but a slightly lower longevity.

Looking at the highest concentration, animals previously exposed to nanoZnO and $ZnSO_4$ presented some differences too. Specimens previously exposed to nanoZnO showed the highest reproduction inhibition (the lowest total number of live neonates per female and the lowest mean brood size, Table S2), while animals previously exposed to $ZnSO_4$ mainly presented more effects on longevity (mean difference vs. control of -8.5 ± 1.7 days) than on reproduction.

During the whole life cycle, mothers exposed to nanoZnO generated the highest number of immobile/dead daphnids (ten times higher than the controls), while $ZnSO_4$ treatment did not present significant differences *vs.* control, even if the number of immobile/dead daphnids was higher than in controls.

The whole experiment, with the two planned phases, allowed us discovering several interesting aspects of the chronic toxicity of these two chemical species of Zinc. NanoZnO exposure seemed to cause the most severe effects on reproduction, with the highest reduction of the reproduction

efficiency and possible effect on neonate vitality at the highest concentration. On the contrary $ZnSO_4$ exposure caused more effects on longevity with respect to reproduction. In fact, during the recovery phase, a significant reduction of longevity was obtained at both concentrations, while the total number of live neonates was not statistically different from that recorded in control (Table 1). This was possible because previously exposed animals presented a slightly lower time-between-broads and a slightly higher mean-broad-size, even if both of them were not statistically different from control (Table S2). Despite this higher reproduction investment (or maybe because of this), the whole reproduction efficiency (total number of live neonates per female) did not differ from that of control, due to the reduction in longevity.

3.2. Light microscopy study

Based on the obtained results and given the low levels of exposure, we decided to perform histological and ultrastructural studies only at the highest concentration (0.3 mg Zn/L), so to better detect the possible morphological effects at cellular level. Histological analyses have been performed on samples mainly focusing at gut level, since it has previously demonstrated to represent a preferential entry route for nanoparticles and xenobiotics in general (Elder et al., 2009).

At 48h, control samples show a regular absorptive midgut composed by columnar cells of about 15-20µm in height, lying on a thick basal lamina and with an evident border of microvilli, longer in the anterior part of the midgut. Epithelial cells show characteristic nuclei, located either centrally or basally, and with clearly evident nucleoli. In the lumen, some ingested material is visible (algae and yeast at different stages of digestion). The digestive system is surrounded by smooth muscle tissue, namely the gut muscolaris, which encircles the whole length of the midgut, and which is well visible in all the sections (Fig. 2). In the nanoZnO and $ZnSO_4$ samples, no differences have been detected if compared to controls, the epithelial cells of the midgut from the exposed samples showing the same structural and morphologic characteristics of the unexposed ones. All digestive cells from treated samples maintained their structural integrity resulting well adherent each other. Also nuclei and nucleoli are similar to those from controls both in size, position and shape, and microvilli are thick and regularly arranged as well (Fig. 2C-F).

At 9d, the morphological fields observed in all samples do not show any differences if compared to controls. Even at 21d, which according to the OECD guidelines represents the exposure time for the

chronic reproduction test in *Daphnia* (OECD, 2012), no significant differences have been detected between controls and the exposed groups. Slightly differences have been observed by comparing the height of the digestive cells in the samples from 21d and 48h, the former being higher than the other. Anyway, no pathological features have been detected by light microscopy, and the general morphology of the digestive cells was preserved, being independent upon kind (nanoZnO and $ZnSO_4$) and time of exposure (48h, 9 and 21d).

3.3. Electron microscopy study

More information was expected by TEM analyses, also considering the possibility of recording NPs inside *D. magna* tissues, despite the very low level of exposure. Additionally, considering that no differences between treated and unexposed samples have been recorded by light microscopy, detailed analyses were necessary to compare the possible adverse effects of nanoZnO and $ZnSO_4$ on samples.

Ultrathin sections from controls at 48h, 9 and 21 days showed the typical enterocyte structure, which agreed with the classic description reported by (Quaglia et al., 1976; Santo et al., 2014; Schultz and Kennedy, 1976). Cells showed a well-developed brush border and a cytoplasm rich in organelles, such as mitochondria, endoplasmic reticulum, Golgi apparatus and lysosomes. The numerous mitochondria presented compact and well characterized cristae, and very interestingly, beside mitochondria, a number of others organelles of around 1μm diameter were observed at any time. These structures, more numerous at 9 and 21d than at 48h, showed an inner system of membranes, thus we named them as “lamellar organelles”. They were surprisingly similar to chloroplasts. Indeed the presence of chloroplasts inside the digestive cells of *Daphnia* spp. has already been reported (Chang and Jenkins, 2000). Anyway this very interesting issue was no longer discussed here, since it needed and was worthy of more specific analyses. Figure 3 showed some fields of midgut cells from 21d control samples.

Samples exposed to ZnO NPs showed a general integrity of the midgut enterocytes and little differences have been detected among 48h, 9 and 21d samples. In 48h samples, few ZnO NPs have been observed in the lumen and inside the midgut cells. The number of NPs into epithelial cells increased in 9 and in 21d samples. According to (Mayhew et al., 2009), the average frequency of NPs in cells was calculated in hundreds sections from each sample at 48h, 9 and 21d. At 48h, the mean

frequency of detecting one NP inside a cell section was around 15%, while at 9d it increased to 50-70%, with more NPs in each cell section. In general, the initial portion of the midgut had a higher amount of NPs and ingested materials (algae and yeast), if compared to the final portion. In 21d samples no differences have been observed in comparison to those from 9d.

The increase in the number of the observed NPs from 48h to 9d samples indicated the persistence of at least a good proportion of NPs for more than 48h, while the similar pattern of NPs occurrence in 9 and 21d samples suggested that NPs persistence did not exceed 9d.

Even at 48h but, more frequently, starting by 9d, NPs were observed: *i*) among and inside microvilli (Fig. 4A, B); *ii*) near the upper cell membrane; *iii*) inside the cytoplasm, either bound to the cytoplasmic side of the plasmatic membrane or as free NPs (Fig. 4C, D); *iv*) into mitochondria (Fig. 4E); *v*) in the paracellular space (Fig. 4C); *vi*) near the nuclear envelope (Fig. 4F), and inside the nucleus; *vii*) at the basement membrane level (Fig. 4G); *viii*) in the gut muscolaris and *ix*) in the eggs (Fig. 4H). The zinc composition of these NPs was confirmed by ESI analyses and some example was reported in Figure 5.

Looking at the cell morphology, the only difference detected between exposed and control samples, was the mitochondrial structure, which in samples at 9 and 21d appeared to be affected by NP exposure. Several mitochondria in all samples from these groups showed a disorganization of their cristae, with the presence of empty spaces. In some cases, both the inner and the outer mitochondrial membranes appeared lysed, as the last step of mitochondrial degeneration (Fig. 4D-E).

Differently from ZnO NPs exposure, no damage to mitochondria has been observed in $ZnSO_4$ samples (Fig. 6). On the contrary, a number of empty vacuoles with disorganised membranes have been detected (Fig. 6B). These figures were very similar to the autophagy vacuoles observed by (Santo et al., 2014) after exposure to high concentrations of the same compounds, even if in the present paper they were reduced in size and less frequent.

The potential Zn exposure coming from the internalization on NPs into gut cells can be calculated starting from the average number of NPs recorded into cells, their dimension and thus their volume and mass, in relation to the cell volume. Considering that a gut epithelial cell has a width and a thickness of about 8 µm and a height of 15-20 µm, the cell volume is 1120 μm^3 (8*8*17.5 µm). Because of a section for TEM analysis has a thickness of 60/70nm, the volume observed for each TEM section is near 1/130 of the total cell volume. From this, a mean number of 20 NPs/cell is derived (NPs had a frequency/probability in each section of 15%). Considering that the mean NP diameter is

20 nm (Santo et al., 2014), 20 NPs/cell have a volume of 8.4 x 10^{-5} μm^3, which corresponds to a weight of 47 x 10^{-5} pg (ZnO density = 5.61 pg/μm^3). In a cell volume of 1120 μm^3 the NP concentration becomes 0.042 x 10^{-5} pg/μm^3. This NP concentration corresponds to a potential release of zinc ion of 0.35 mg Zn/L. Obviously, NPs observed at TEM were not dissolved, but these calculations are proposed in order to demonstrate that the dissolution of 20 NPs would be able to cause a quite high intra-cellular Zinc concentration. It is interesting noting that this concentration is similar to that of the soluble salt in the exposure media (0.3 mg Zn/L), which is unable to cause swelling of mitochondria. ZnO NPs did not cause this effect at 48h, but later when the NP number increased (9-21d) this happened. Considering that at 9 and 21d, NPs were much more frequent, the potential Zn concentration inside cells could be even higher.

4. Discussion

This work aimed to evaluate the chronic effects of low concentrations of ZnO NPs in comparison to the soluble Zinc, $ZnSO_4$. So far, three papers have studied the chronic toxicity of ZnO NPs on *D. magna* (Adam et al., 2014; Lopes et al., 2014; Zhao et al., 2012), but none has compared the chronic effects of ZnO NPs and soluble zinc by a morphological approach. Advance microscopic techniques have been here applied in order to detect and visualize the possible NPs internalization without huge contaminations, which are typical of acute toxicity exposures. Moreover, such an approach was also used to compare the effects of NPs and soluble salt on young and adults, for a better understanding of the toxicity mechanism of nanoZnO. Thus, the experimental plan of the present paper was specifically performed to obtain samples for the microscopic analyses, and not to gain those ecotoxicological parameters, such as NOEC, LOEC or EC_{50}, which have already been determined for *D. magna* and available in literature.

4.1. Life cycle parameters: comparison between nanoparticles vs. soluble Zn

Nominal concentrations for both $ZnSO_4$ and ZnO (0.1 and 0.3 mg Zn/L) were selected near and slightly above the EC_{50} values for chronic toxicity of these compounds on *D. magna*, as reported by (Adam et al., 2014): EC_{50} of 0.11 and 0.082 mg Zn /L for ZnO NPs and $ZnCl_2$, respectively. These

concentrations are more realistic than those of acute toxicity, even if they are still far from the environmental concentrations given for ZnO NPs in natural waters, and which stay in the order of ng/L (Gottschalk et al., 2009). During exposure, the analytically-determined median concentrations of soluble Zn were lower than nominal ones, especially for the nanoparticulate form (<0.0084 and 0.059 mg Zn/L for nanoZnO at 0.1 and 0.3 mg Zn/L, respectively). Measured median concentrations of Zn ions for the soluble form ($ZnSO_4$) were at least three times higher (0.022 and 0.16 mg Zn/L at 0.1 and 0.3 mg Zn/L, respectively). Therefore, if toxic effects would come from soluble ions in the exposure medium, they should be greater for $ZnSO_4$ than for nanoZnO. Our data supported the hypothesis of a specific toxicity coming from the nanoparticulate form (ingestion of NPs and later events).

Looking at the toxicity levels of the to forms of Zn, the reproduction inhibition observed for both compounds (around 0.1 mg Zn/L) well agreed with results from (Adam et al., 2014) and (Lopes et al., 2014), while the range of chronic toxicity reported by (Zhao et al., 2012) was much lower than that observed in the present study.

The novelty of this work was the study of the recovery phase, after exposure. Detoxification and full-reproduction recovery were quite different among treatments, giving in one case a total reproduction even higher than that observed in control (exposure to nano ZnO at the lowest concentration). In this case, the higher reproduction potential was achieved by a positive effect on longevity. Interestingly, we observed at 21d an evident reduction of adult size only in samples exposed to ZnO NPs. Adam and colleagues too (Adam et al., 2014), observed a higher reduction in size in samples exposed to ZnO NPs (reduction of 12% in relation to control) *versus* those exposed to $ZnCl_2$ (2%). Basing on these evidences, we hypothesized that size reduction, specifically induced by the nanoparticulate form, was due to a slackening in the growth rate, which indirectly determined a higher longevity, once exposure was suspended. After a detoxification phase (first period after exposure), the reproductive potential was fully recovered, and the higher longevity (64 days *vs.* 57 of control) allowed adults to have a higher number of broads (18.2 *vs.* 15.2 in control), determining a total reproduction even higher than that registered in control (437 live neonates per female *vs.* 389 in control).

In literature, the comparison between soluble and nanoZn toxicity was exclusively studied by exposure trials; on the contrary our experiments, introducing the recovery phase, revealed important differences on the toxicity of the two form of Zn, even on life traits: nano ZnO showed a higher effect on reproduction (maximal inhibition during exposure), while soluble Zn specifically acted on longevity

(reducing longevity at both concentrations). The explanation of this may derive by the interpretation of the mechanism of action of these two forms of Zn. First at all, it must be consider the role of Zn ions, which are also present after addition of nanoZnO. In literature, the role of zinc ions in ZnO NPs toxicity is still a very debated point. Several papers reported that ZnO NPs toxicity was due not only to the solubilized ions, whose effects were different from those due to NPs (Bai et al., 2010; Hao et al., 2013; Poynton et al., 2011; Xiao et al., 2015); others strongly suggested that ZnO NPs toxicity was caused solely by them (Adam et al., 2014; Adam et al., 2015; Heinlaan et al., 2008). The relative toxicity of zinc ions directly released from ZnO NPs was recently studied by Xiao and co-workers (Xiao et al., 2015) who concluded that only 30% of the acute toxicity of ZnO NPs was due to released ions. The same authors reported that the role of dissolved ions may be different depending on concentration: at high concentrations (acute toxicity range) particles rather than Zn ions were the major source of toxicity, while at low concentrations (chronic range) the dissolved ions could be predominant. Bacchetta et al. (2016), by the same morfological approach used in this paper, concluded that the nano ZnO toxicity (at high concentrations) was mainly due to Zn ions, released inside cells by internalized NPs. A crucial point for establishing the role of solubilised ions in the ZnO NPs toxicity is the amount and velocity of ZnO NPs solubilisation. If the solubilisation is fast and almost complete, the possibility of a specific toxicity due to NPs become improbable, while if NPs persist longer, the possibility of specific effects of NPs is higher, and the toxicity can be either due to NPs themselves or to the *in-situ* solubilised ions. Unfortunately, solubilisation of ZnO NPs is far from being completely understood because it is greatly affected by many variables, such as coating, size and concentration, as well as by the medium characteristics such as pH and ionic strength. Adam and colleagues (Adam et al., 2014) reported that at low concentrations, namely in the range of the chronic toxicity, most of the ZnO NPs, even if aggregated, dissolved within 48h (average of 90.9 ± 2.5%), and according to (Xiao et al., 2015), they additionally showed that the dissolution was quite rapid (60% in 1-2h). At higher concentration ranges, ZnO NP solubility seemed to behave differently, with levels of solubilisation definitively lower and in the range of 4-18% (Poynton et al., 2011; Santo et al., 2014; Wang et al., 2009). According to the literature, the amount and proportion of solubilized ions in the test medium change greatly depending on the test conditions. The final concentration in the medium should be theoretically near the ZnO equilibrium solubility, thus the amount of the ZnO NPs solubilized can vary dramatically: from irrelevant fractions, when exposure concentrations are much above the

equilibrium solubility, to nearly the whole amount, when exposure concentrations approach the maximum solubility. Our analytical results showed that, even at the lowest concentrations (0.1 mg Zn/L), the solubilized ions were limited to a fraction (<10% of total amount of Zn). In these conditions, ZnO NP can enter the digestive tract of *D. magna* and can be internalized in tissues and cells. Differently from the soluble form, ZnO NPs have the specific role in physically carrying consistent Zinc amount into the organism, which in turn can locally increase ions concentration by intra-cellular solubilisation (Bacchetta et al., 2016). As discussed in the next paragraph, we hypothesized that the amount of Zn ions carried inside tissues and cells differed between the two chemicals, the nanoparticulate form being able to accumulate high intracellular Zn ions concentration by a secondary ions release subsequent to NP internalization.

Another interesting difference between NP and soluble Zn toxicity deals with the number of immobilized/dead daphnids observed in the nanoZnO and $ZnSO_4$ exposed groups and the time at which these specimens have been detected (end of exposure and immediately after it). These findings supported the conclusion that the effects on daphnids were not caused by a direct toxicity coming from the exposure media, but by an indirect toxicity coming from the mothers. In the first case in fact, daphnid immobilisation should have happened during the whole exposure phase, and should have stopped immediately after it. The finding that immobile samples have been mainly observed in the offspring of nanoZnO exposed groups and only at the end of the exposure period as well as in the first detoxification phase, supported the hypothesis that such an effect was mediated from mothers and was determined by the accumulation of NPs during exposures. This explanation was also supported by the detection, confirmed by ESI analysis, of many NPs within the eggs (Fig. 4H). Indeed, many nanomaterials, such as Au, TiO_2, SiO_2, polystyrene, quantum dots and carbon NPs, could penetrate the placental barrier (Chu et al., 2010; Sun et al., 2013), and some studies reported that e.g. TiO_2 NPs could cross even the blood–brain barrier (Wang et al., 2008). In this light, our finding is not surprising, even if never documented or reported before in *Daphnia* sp. Independently where these NPs have come from, and how they have reached the ovary, the risk associated to maternal exposure in offspring is clear. Takeda and co-workers (Takeda et al., 2009) demonstrated that TiO_2 NPs could be transferred from mother to offspring, damaging their reproductive and nervous systems. Also ZnO NPs have been reported to accumulate in mammary tissue of dams, as well as in kidney and liver of pups (Jo et al., 2013). These authors hypothesized that trans-placental and breastfeeding transport of ZnO

nanomaterial actively occurred between pregnant mother and pups and concluded that even if fertility and mating parameters were unaffected by nanoZnO treatment, dams exposed to NPs before pregnancy and during gestation and lactation led to clear indications of developmental toxicity in the offspring (Jo et al., 2013). Of course multi-generation investigations are needed to fully understand the risk associated to maternal exposure to NPs, but from the increasing number of paper on the topic it is clear that the interest of the scientific community towards this issue is far from being completely satisfied.

4.2. Microscopic analyses: comparison between nanoparticles vs. soluble Zn

Histological analyses didn't reveal any differences between the two compounds or between them and the controls, but images from ultrathin sections showed interesting discrepancies: first of all, the finding of ZnO NPs inside cells. Given the feeding behaviour of the species, the probability to find NPs in the digestive tract was high, but the possibility to detect them into cells was quite faint, considering the low level of exposure and the high solubility of ZnO NPs at low concentrations, as suggested by some authors (Adam et al., 2014). The finding of NPs inside different cell compartments of the digestive tract, and even outside it (presence confirmed by ESI analyses) was a key point for interpreting toxicity events, because it demonstrated that at least some NPs were able to be internalized in the cells of different tissues and to persist there in the nanoparticulate form. According to the findings of several authors (Bacchetta et al., 2012; Frohlich and Roblegg, 2012; Verma et al., 2008), the recent work of Santo and colleagues (Santo et al., 2014) described two possible internalization pathways: *i*) crossing through the cell membrane without disruption, mainly via the microvilli, and *ii*) following the endocytic pathway. Uptake by the microvilli was already reported also by (Harush-Frenkel et al., 2008) and by (Lovern et al., 2008) *in vitro* and *in vivo*, as well as the translocation of NPs outside the epithelial barrier (Bacchetta et al., 2012; Santo et al., 2014), but in all these cases the concentrations of ZnO NPs were high. The presence of NPs among and inside the microvilli (Fig. 4A-B) as well as their detection in the cytoplasm and paracellular spaces (Fig. 4B-D), confirmed the aforementioned entry routes and showed for the first time that also at low concentrations ZnO NPs can be internalized by enterocytes and can pass the epithelial barrier reaching other body districts.

The entry of NPs into cells gave an additional evidence of a possible specific toxicity due to the nanoparticulate form, and ultrastructural analyses of the midgut enterocytes supported once more this hypothesis. Mitochondria from samples exposed to ZnO NPs showed several damages, while those from $ZnSO_4$ did not. Many authors reported that mitochondria represented target organelles for ZnO NPs: Santo and colleagues (Santo et al., 2014) observed swollen mitochondria in the cytoplasm of the digestive cells of *D. magna* exposed to nanoZnO identical to those observed here (Fig. 7A-B). According to other authors (Pi et al., 2013; Poynton et al., 2011; Zhu et al., 2009), they hypothesized that NPs induced mitochondrial damage via oxidative stress. Also Wiseman reported that ZnO NPs exposure led to mitochondria damage through ROS generation (Wiseman et al., 2007), and Xia (Xia et al., 2008) reported that metal oxide NPs, internalized into mitochondria, were able to produce locally soluble ions, which in turn induced the disruption of the organelles and triggered ROS generation. The same mechanism was demonstrated in the enterocytes of the amphibian *Xenopus laevis* exposed to ZnO NPs (Bacchetta et al., 2014), as well as in isolated rat liver mitochondria exposed to the same NPs (Li et al., 2003). However, the effects on mitochondria via oxidative stress caused by ROS production seemed to be a well-established toxic mechanism linked not only to ZnO NPs exposure, but also to soluble zinc (Cheng et al., 2010). Indeed, degeneration of mitochondria can be the common effect of ZnO NPs and $ZnSO_4$, (Bacchetta et al., 2016) but as reported above, at low concentrations damages to mitochondria were observed only after ZnO NPs exposure, and not after $ZnSO_4$ one. We believed that at low levels of exposure, only ZnO NPs were able to produce a zinc ions concentration sufficient to trigger the mitochondrial degeneration process. It is interesting noting that this effect was observed only at 9 and 21d, when evidences of NPs accumulation into epithelial cells were obtained. Adam et al. (2014) reported that the amount of Zn accumulated in organisms from NP exposure was similar to that coming from the exposure to the same concentration of soluble Zn (Zn ions from $ZnCl_2$), while Xiao et al. (2015) showed that the amount of Zn in organisms from NP exposure was higher than that coming from ions solubilised in the test medium from the corresponding ZnO NP concentration. These studies, apparently in contrast each other, actually tested different hypotheses, but they were unable to verify the effective accumulation of NPs inside the organism, because they measured total Zn concentration (sum of NPs and ions). Our work demonstrated that NP internalisation has already occurred at 48h and that NP accumulation continued at least until 9d. After this time a sort of plateau was reached in the NPs detection frequencies inside epithelial cells.

We hypothesized that this NPs accumulation was able to produce a Zn ion concentration sufficient to produce the observed effects on mitochondria by day 9. According to this hypothesis, our $ZnSO_4$ exposures were unable to produce such an effect, while higher did. A very recent research (Bacchetta et al., 2016) reported that high concentrations of $ZnSO_4$ caused not only swollen mitochondria, but also the appearance of degenerative figures in the cytoplasm of the digestive cells, such as autophagy vacuoles. In the present paper, these last figures have been observed in samples exposed to low $ZnSO_4$ concentrations (Fig. 7C), and were morphologically identical to those observed after high $ZnSO_4$ exposure, even if reduced in size and frequency (Fig. 7D). These figures are linked to cellular aging phenomena, as well documented in literature (Lipetz and Cristofalo, 1972). This last finding, extrapolated to the individual level, accords with the observed effect on longevity, which appeared to be specific of $ZnSO_4$ exposure.

5. Conclusions

The present work studied the chronic effects of ZnO NPs and $ZnSO_4$ exposure on *D. magna* also beyond the standard 21-day-exposure time and throughout the whole life cycle. TEM analyses demonstrated that at low concentrations insolubilized NPs did exist inside the gut, the epithelial cells and even the tissues beyond the epithelial barrier. NPs number increased from 48h until 9d, demonstrating the accumulation and persistence of NPs into *D. magna* tissues. Between 9 and 21d, NPs number did not increase, likely depending from two processes: *i)* the solubilisation of NPs inside cells, determining citotoxicity; *ii)* translocation to other body districts, with possible effects outside the midgut. Many NPs were observed in the ovary within eggs and, besides their fate has not been investigated further, a high number of immobilized daphnids were observed only after ZnO NPs exposure, and only at the end of the exposure period (21d). This suggested that effects on daphnids were caused by the chronic accumulation of NPs in mothers with a translocation to reproductive cells (transfer of the contamination from the mothers to the offspring). Such an issue is worthy of more detailed studies, and raises concerns about the risk associated to an uncontrolled use of NPs.
Both ultrastructural observations and macroscopic effects on fitness during the whole life cycle indicated different toxicity effects between the two compounds, at least at low concentrations. We

believed that ZnO NPs ingested by *D. magna* were able to carry an amount of zinc higher than that provided by the soluble form, and sufficient to cause a direct damage to mitochondria. This would be responsible for low energy availability at body level and for the consequent reduction of growth and reproduction. Differently from NPs, $ZnSO_4$ exposed samples did not show any evident growth reduction, but a lower reproduction and a reduced longevity. Our morphological analyses, which revealed the presence of figures linked to the physiological process of cellular aging, suggested that the observed reduction of longevity could be related to an accelerated cellular aging phenomenon. Under this condition, cell efficiency may be reduced (lower reproduction than the control) and the life cycle shortened (lower longevity than the control). Thus, at low concentrations ZnO NPs determined effects different from those due to the same amount of soluble zinc, macroscopically on the life cycle parameters and microscopically on the epithelial cell ultrastructure. We believe that these differences derived from the ability of NPs of carrying into specific cells and tissues a higher amount of Zn than the corresponding soluble form, by the combination of an efficient NP internalisation and accumulation phenomena. These considerations led to the conclusion that Zn ions still play a key role on ZnO cytotoxicity, but that NPs are able to cause specific toxic effects because of their capacity of efficient carriers of soluble ions into cells.

Acknowledgements

Authors would like to thank Dr Maria Carla Panzeri and Dr Paola Podini for their technical help and for the facilities they kindly provided. Authors are also grateful to B.A. Maria Luisa Bonicalzi for help maintaining daphnid cultures, and to three anonymous reviewers for their constructive comments, which helped to improve the manuscript.

References

Adam, N., et al., 2014. The chronic toxicity of ZnO nanoparticles and $ZnCl_2$ to *Daphnia magna* and the use of different methods to assess nanoparticle aggregation and dissolution. Nanotoxicology. 8**,** 709-717.

Adam, N., et al., 2015. Gene transcription patterns and energy reserves in *Daphnia magna* show no nanoparticle specific toxicity when exposed to ZnO and CuO nanoparticles. Environmental Research. 138**,** 82-92.

Aruoja, V., et al., 2009. Toxicity of nanoparticles of CuO, ZnO and TiO_2 to microalgae *Pseudokirchneriella subcapitata*. Science of the Total Environment. 407**,** 1461-1468.

Bacchetta, R., et al., 2016. Role of soluble zinc in ZnO nanoparticle cytotoxicity in *Daphnia magna*: A morphological approach. Environmental Research. 148**,** 376-385.

Bacchetta, R., et al., 2014. Evidence and uptake routes for Zinc oxide nanoparticles through the gastrointestinal barrier in *Xenopus laevis*. Nanotoxicology. 8**,** 728-744.

Bacchetta, R., et al., 2012. Nano-sized CuO, TiO_2 and ZnO affect *Xenopus laevis* development. Nanotoxicology. 6**,** 381-398.

Bai, W., et al., 2010. Toxicity of zinc oxide nanoparticles to zebrafish embryo: a physicochemical study of toxicity mechanism. Journal of Nanoparticle Research. 12**,** 1645-1654.

Chang, N., Jenkins, D. G., 2000. Plastid endosymbionts in the freshwater crustacean *Daphnia obtusa*. Journal of Crustacean Biology. 20**,** 231-238.

Cheng, W. Y., et al., 2010. An Integrated Imaging Approach to the Study of Oxidative Stress Generation by Mitochondrial Dysfunction in Living Cells. Environmental Health Perspectives. 118**,** 902-908.

Chu, M., et al., 2010. Transfer of quantum dots from pregnant mice to pups across the placental barrier. Small. 6**,** 670-678.

David, C. A., et al., 2012. Dissolution Kinetics and Solubility of ZnO Nanoparticles Followed by AGNES. Journal of Physical Chemistry C. 116**,** 11758-11767.

Elder, A., et al., 2009. Physicochemical factors that affect metal and metal oxide nanoparticle passage across epithelial barriers. Wiley Interdisciplinary Reviews-Nanomedicine and Nanobiotechnology. 1**,** 434-450.

Farre, M., et al., 2009. Ecotoxicity and analysis of nanomaterials in the aquatic environment. Analytical and Bioanalytical Chemistry. 393**,** 81-95.

Franklin, N. M., et al., 2007. Comparative toxicity of nanoparticulate ZnO, bulk ZnO, and $ZnCl_2$ to a freshwater microalga (*Pseudokirchneriella subcapitata*): The importance of particle solubility. Environmental Science & Technology. 41**,** 8484-8490.

Frey, D. G., 1982. Contrasting strategies of gamogenesis in Northern and Southern populations of Cladocera Ecology. 63**,** 223-241.

Frohlich, E., Roblegg, E., 2012. Models for oral uptake of nanoparticles in consumer products. Toxicology. 291**,** 10-17.

Gottschalk, F., et al., 2009. Modeled Environmental Concentrations of Engineered Nanomaterials (TiO_2, ZnO, Ag, CNT, Fullerenes) for Different Regions. Environmental Science & Technology. 43**,** 9216-9222.

Hao, L. H., et al., 2013. Bioaccumulation and sub-acute toxicity of zinc oxide nanoparticles in juvenile carp (*Cyprinus carpio*): A comparative study with its bulk counterparts. Ecotoxicology and Environmental Safety. 91**,** 52-60.

Harush-Frenkel, O., et al., 2008. Surface charge of nanoparticles determines their endocytic and transcytotic pathway in polarized MDCK cells. Biomacromolecules. 9**,** 435-443.

Heinlaan, M., et al., 2008. Toxicity of nanosized and bulk ZnO, CuO and TiO_2 to bacteria *Vibrio fischeri* and crustaceans *Daphnia magna* and *Thamnocephalus platyurus*. Chemosphere. 71**,** 1308-1316.

Jo, E., et al., 2013. Exposure to zinc oxide nanoparticles affects reproductive development and biodistribution in offspring rats. Journal of Toxicological Sciences. 38**,** 525-530.

Kahru, A., Dubourguier, H. C., 2010. From ecotoxicology to nanoecotoxicology. Toxicology. 269**,** 105-119.

Li, N., et al., 2003. Ultrafine particulate pollutants induce oxidative stress and mitochondrial damage. Environmental Health Perspectives. 111**,** 455-460.

Lipetz, J., Cristofalo, V. J., 1972. Ultrastructural changes accompanying the aging of human diploid cells in culture. J Ultrastruct Res. 39**,** 43-56.

Lopes, S., et al., 2014. Zinc Oxide Nanoparticles Toxicity to *Daphnia Magna*: Size-Dependent Effects and Dissolution. Environmental Toxicology and Chemistry. 33**,** 190-198.

Lovern, S. B., et al., 2008. Electron microscopy of gold nanoparticle intake in the gut of *Daphnia magna*. Nanotoxicology. 2**,** 43-48.

Mayhew, T. M., et al., 2009. A review of recent methods for efficiently quantifying immunogold and other nanoparticles using TEM sections through cells, tissues and organs. Annals of Anatomy-Anatomischer Anzeiger. 191**,** 153-170.

OECD, 2012. Test No. 211: *Daphnia magna* Reproduction Test. OECD Publishing.

Pi, J., et al., 2013. Pathway of cytotoxicity induced by folic acid modified selenium nanoparticles in MCF-7 cells. Applied Microbiology and Biotechnology. 97**,** 1051-1062.

Poynton, H. C., et al., 2011. Differential Gene Expression in *Daphnia magna* Suggests Distinct Modes of Action and Bioavailability for ZnO Nanoparticles and Zn Ions. Environmental Science & Technology. 45**,** 762-768.

Quaglia, A., et al., 1976. Studies on the intestine of Daphnidae (Crustacea, Cladocera) ultrastructure of the midgut of *Daphnia magna* and *Daphnia obtusa*. Journal of Morphology. 150**,** 711-725.

Santo, N., et al., 2014. Toxic effects and ultrastructural damages to *Daphnia magna* of two differently sized ZnO nanoparticles: Does size matter? Water Research. 53**,** 339-350.

Schultz, T. W., Kennedy, J. R., 1976. The fine structure of the digestive system of *Daphnia pulex* (Crustacea: Cladocera). Tissue Cell. 8**,** 479-490.

Sun, J., et al., 2013. Effects of nanotoxicity on female reproductivity and fetal development in animal models. International Journal of Molecular Sciences. 14**,** 9319-9337.

Takeda, K., et al., 2009. Nanoparticles Transferred from Pregnant Mice to Their Offspring Can Damage the Genital and Cranial Nerve Systems. Journal of Health Science. 55**,** 95-102.

Vaseem, M., et al., ZnO Nanoparticles: Growth, Properties, and Aplications. In: A. Umar, Y.-B. Hahn, Eds.), Metal Oxide Nanostructures and their Applications. American Scientific Publishers, Los Angeles, USA, 2010, pp. 1-36.

Verma, A., et al., 2008. Surface-structure-regulated cell-membrane penetration by monolayer-protected nanoparticles. Nature Materials. 7**,** 588-595.

Wang, H. H., et al., 2009. Toxicity of nanoparticulate and bulk ZnO, Al_2O_3 and TiO_2 to the nematode *Caenorhabditis elegans*. Environmental Pollution. 157**,** 1171-1177.

Wang, J. X., et al., 2008. Time-dependent translocation and potential impairment on central nervous system by intranasally instilled TiO_2 nanoparticles. Toxicology. 254**,** 82-90.

Wiench, K., et al., 2009. Acute and chronic effects of nano- and non-nano-scale TiO_2 and ZnO particles on mobility and reproduction of the freshwater invertebrate *Daphnia magna*. Chemosphere. 76**,** 1356-1365.

Wiseman, D. A., et al., 2007. Alterations in zinc homeostasis underlie endothelial cell death induced by oxidative stress from acute exposure to hydrogen peroxide. American Journal of Physiology-Lung Cellular and Molecular Physiology. 292**,** L165-L177.

Xia, T., et al., 2008. Comparison of the Mechanism of Toxicity of Zinc Oxide and Cerium Oxide Nanoparticles Based on Dissolution and Oxidative Stress Properties. Acs Nano. 2**,** 2121-2134.

Xiao, Y. L., et al., 2015. Toxicity and Accumulation of Cu and ZnO Nanoparticles in *Daphnia magna*. Environmental Science & Technology. 49**,** 4657-4664.

Zhao, H.-z., et al., 2012. Toxicity of nanoscale CuO and ZnO to *Daphnia magna*. Chem. Res. Chinese Universities. 28**,** 209-213.

Zhu, X. S., et al., 2009. The impact of ZnO nanoparticle aggregates on the embryonic development of zebrafish (*Danio rerio*). Nanotechnology. 20**,** 195103.

Table 1

Table 1. Total number of live and immobile/dead neonates per female ± standard deviation during exposure phase, recovery phase and whole life cycle for exposed and control groups at the two tested concentrations (0.1 and 0.3 mg Zn/L). Longevity is reported in days with 95% confidence interval. Letters indicate significant differences between treatment with $p<0.05$

Treatment	Concentration	Exposure 0-21 days		Recovery 21 day-end of life cycle		Whole life cycle 0 day-end of life cycle		Longevity
		live neonates per female	dead neonates per female	live neonates per female	dead neonates per female	live neonates per female	dead neonates per female	
	(mg Zn/L)							(days)
CTL-1	-	66 ± 6.6 a	-	323 ± 15 b	-	389 ± 15 b	-	57 (53-59) b
nZnO	0.1	35 ± 15 b	-	402 ± 20 a	-	437 ± 20 a	-	64 (61-66) a
$ZnSO_4$	0.1	49 ± 6 b	-	315 ± 24 b	-	364 ± 24 b	-	54 (52-56) c
CTL-2	-	70 ± 12 a	-	328 ± 38 a	0.5 ± 1.0	398 ± 38 a	0.5 ± 1.0 b	61 (59-62) a
nZnO	0.3	19 ± 3.4 c	3.2 ± 3.0	232 ± 21 b	1.8 ± 1.0	251 ± 21 b	5.0 ± 2.0 a	56 (53-58) b
$ZnSO_4$	0.3	40 ± 6.2 b	0.5 ± 0.5	308 ± 31 a	1.5 ± 2.0	348 ± 31 a	2.0 ± 2.0 b	53 (50-54) c

Figure 1

Click here to download high resolution image

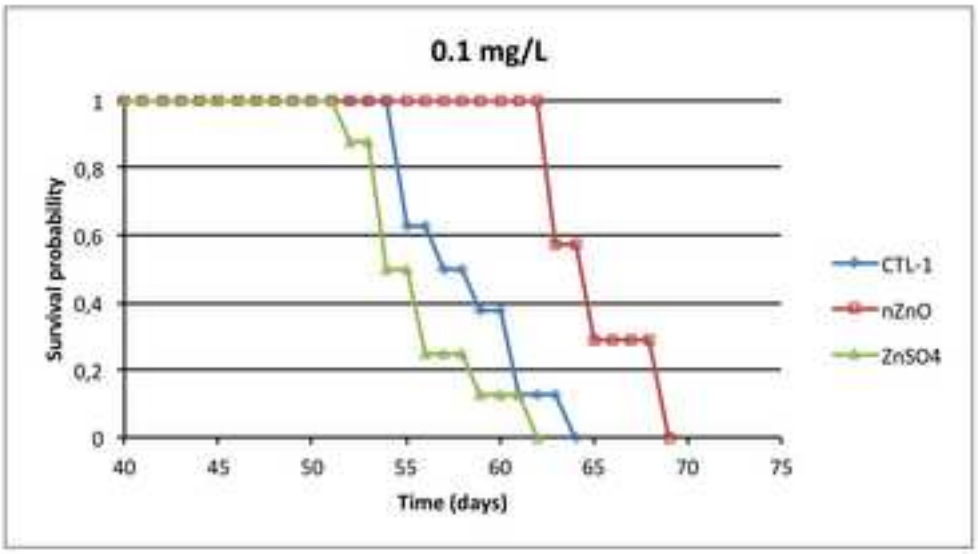

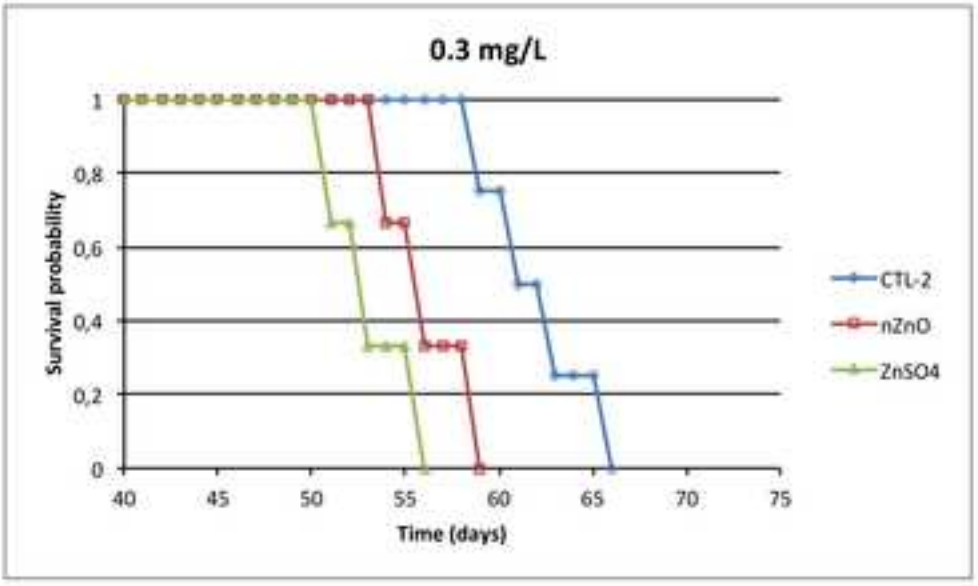

Figure 2

Click here to download high resolution image

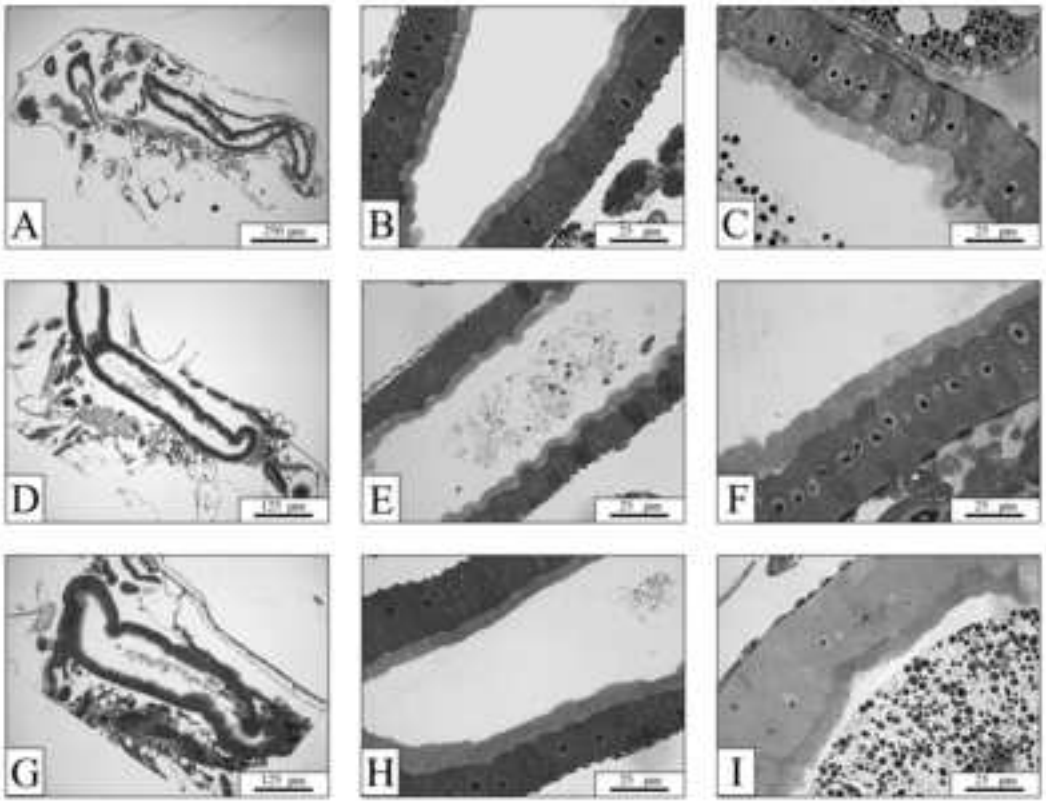

Figure 3

Click here to download high resolution image

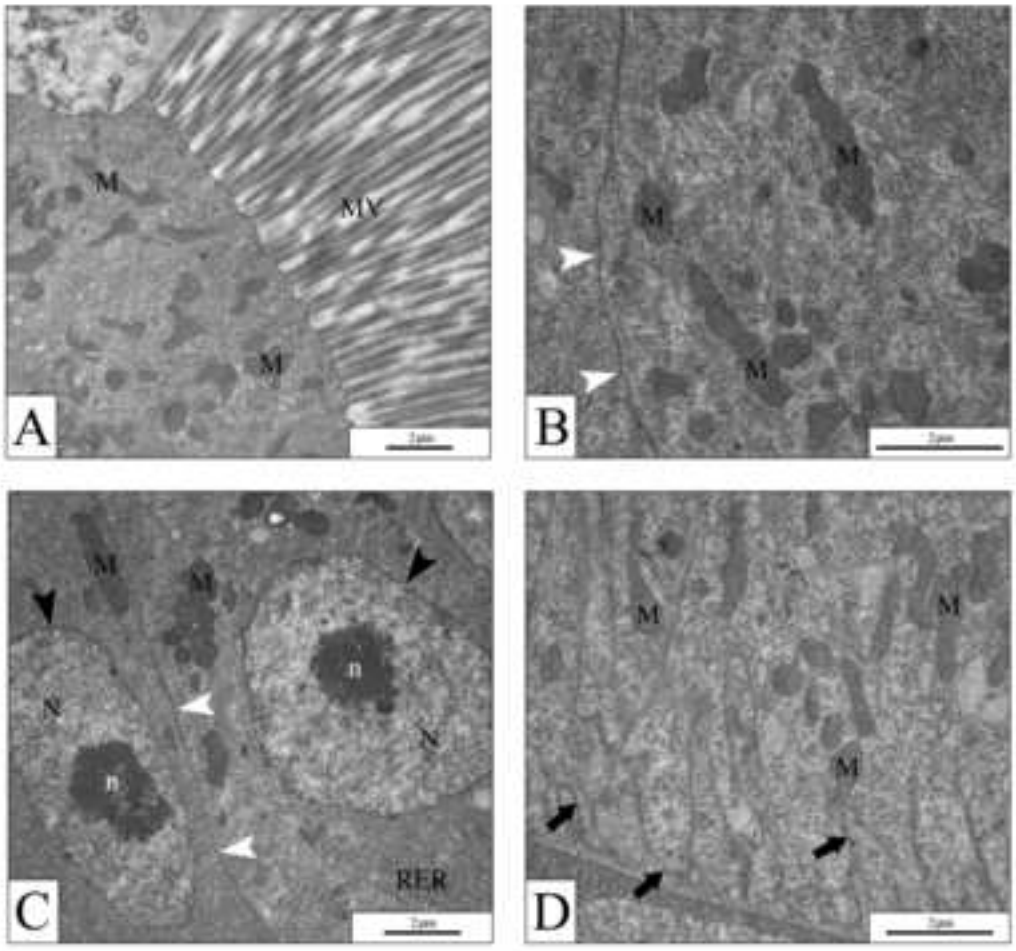

Figure 4

Click here to download high resolution image

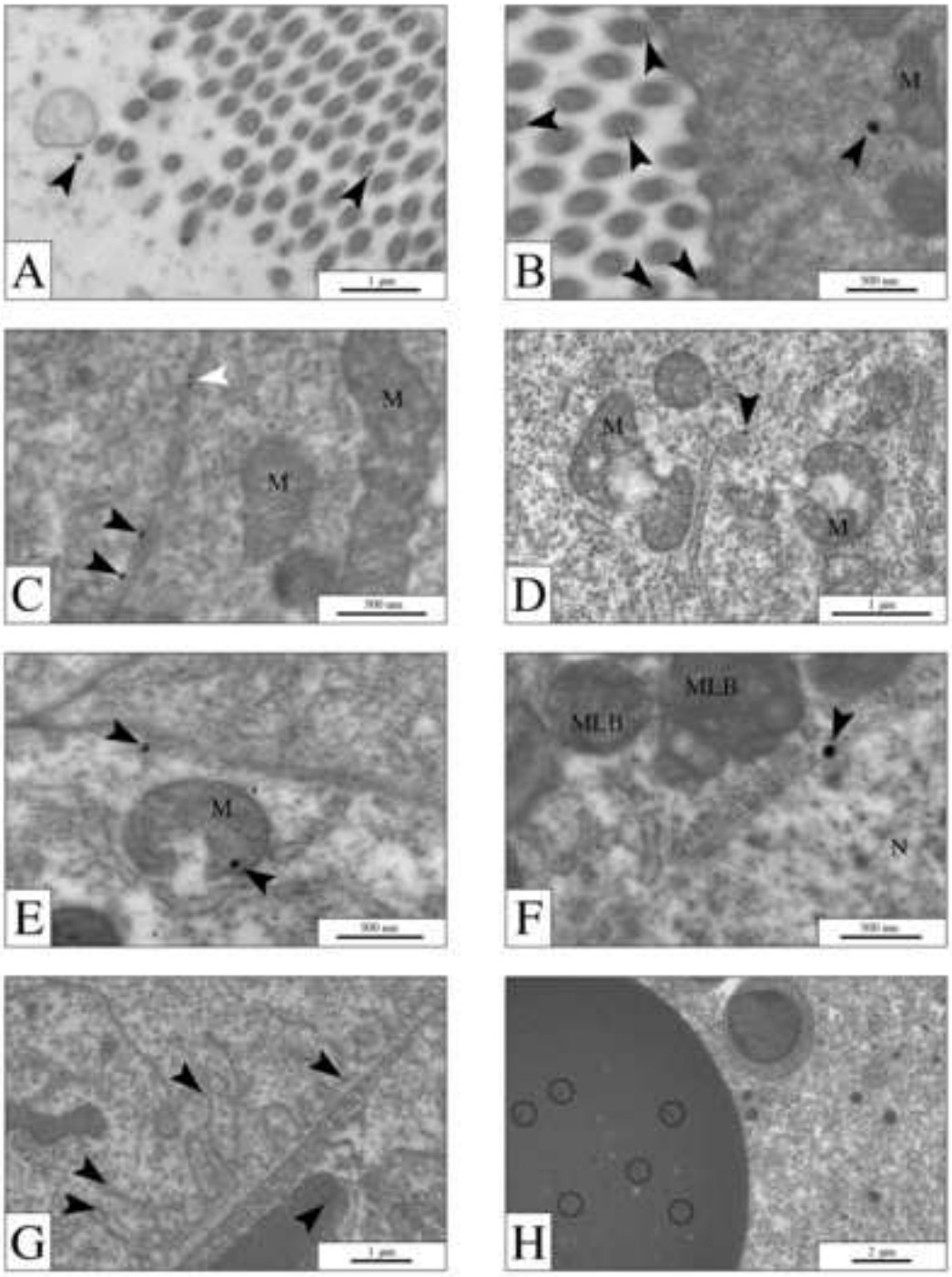

Figure 5

Click here to download high resolution image

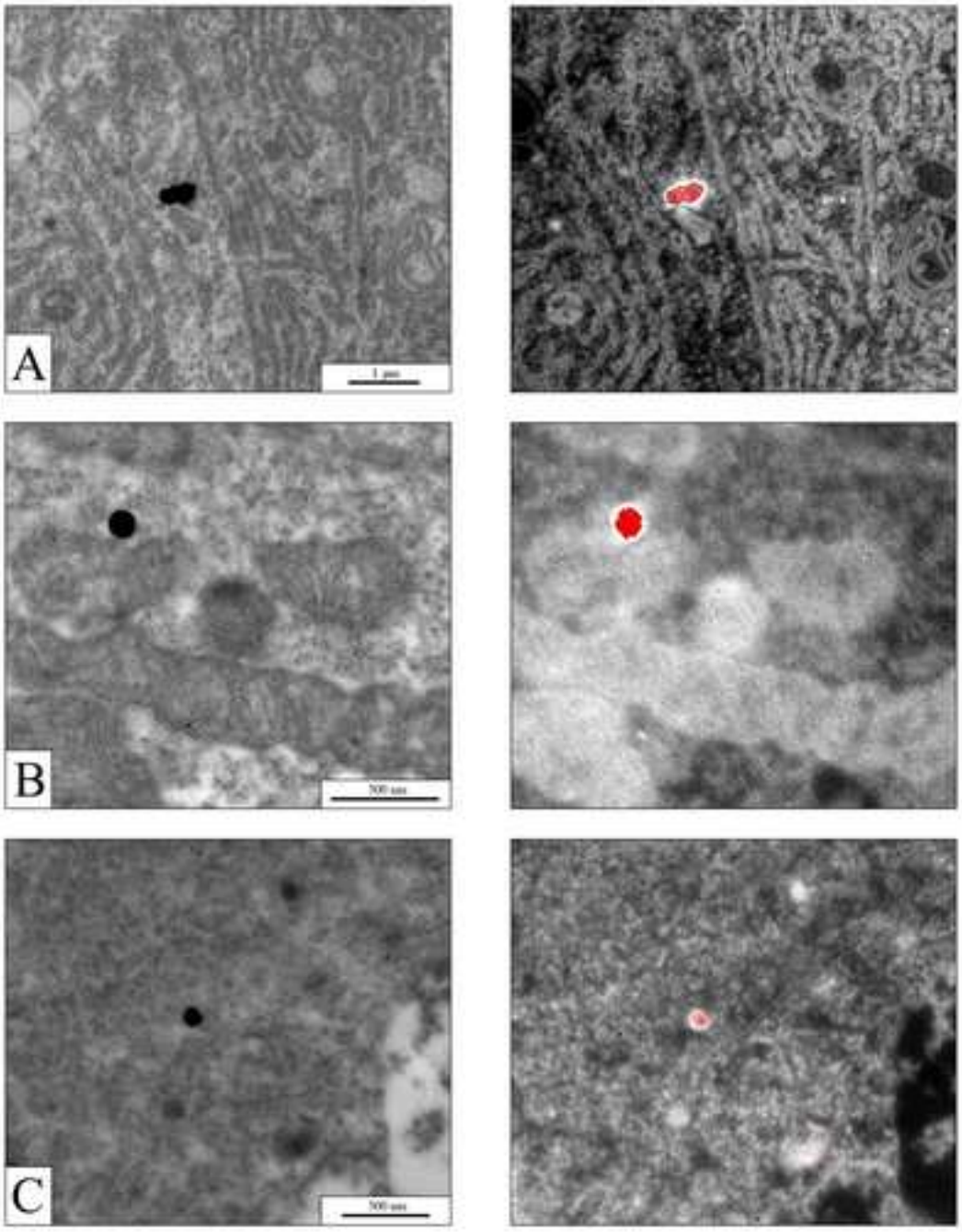

Figure 6

Click here to download high resolution image

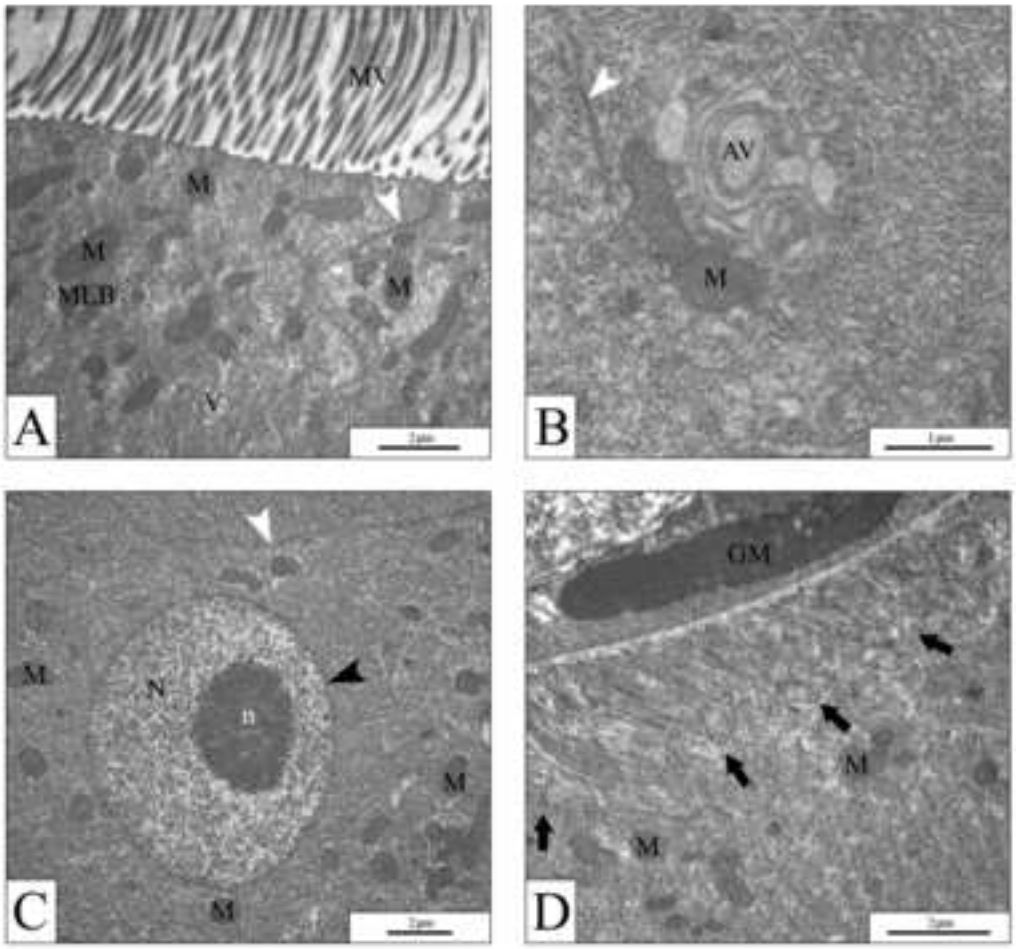

Figure 7

Click here to download high resolution image

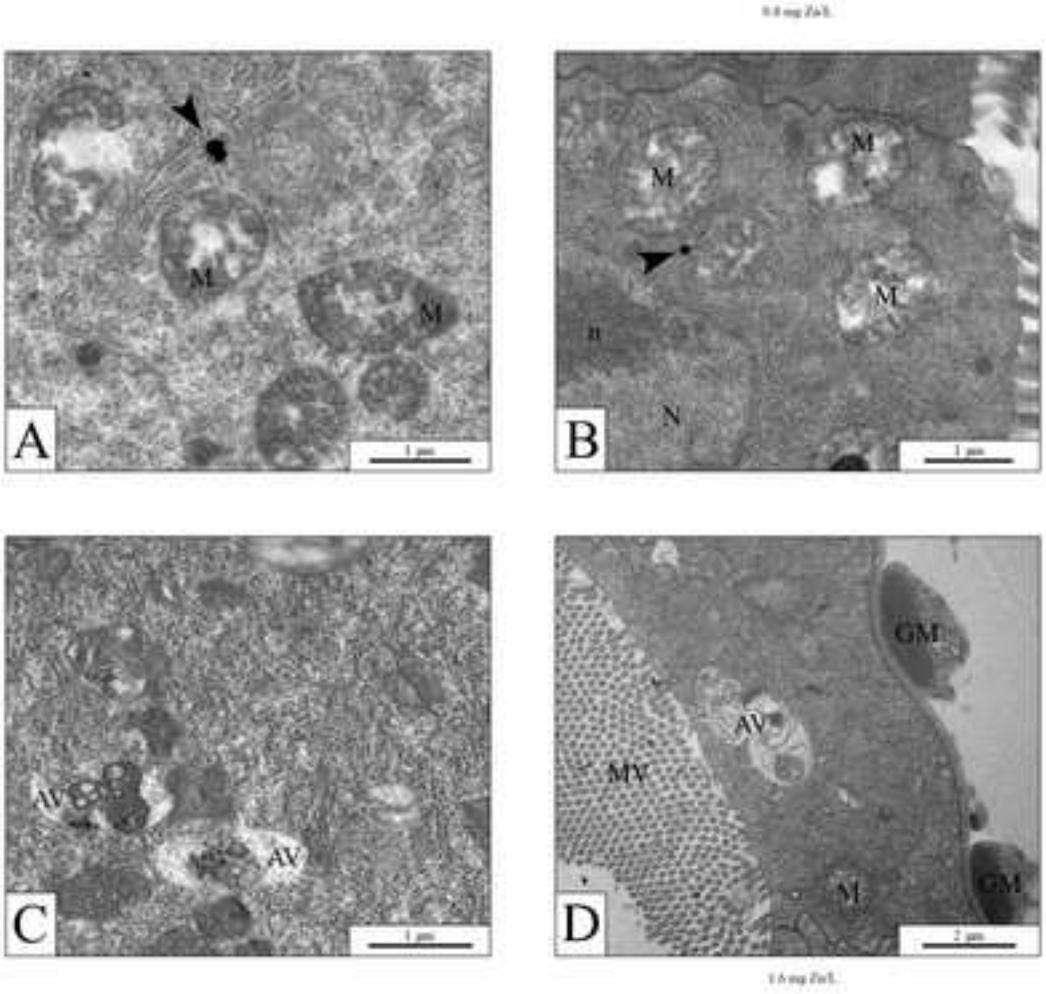

Figure captions

Click here to download Supplementary Material: Figure captions.doc

Table S1

Click here to download Supplementary Material: Table S1.xlsx

Table S2

Click here to download Supplementary Material: Table S2.xlsx

Graphical Abstract

Click here to download Supplementary Material: Graphical Abstract.jpg

Author Addition 1

Click here to download Supplementary Material: Author addition_coauthors.jpg

Author Addition 2

Click here to download Supplementary Material: Author addition_Marelli.doc